Nanosecond Transient Spectroscopy on Conjugated Polymers

Diplomarbeit zur Erlangung des akademischen Grades

Diplom Ingenieur

im Diplomstudium

Technische Chemie

angefertigt am

Linz Institute for Organic Solar Cells (LIOS)

eingereicht von

Anita Fuchsbauer

unter der Betreuung von

o. Univ. Prof. Dr. Serdar N. Sariciftci

Linz, Juli 2005

Zusammenfassung

Das Ziel dieser Arbeit war es das auf dem Institut neu erworbene Spektrometer mit Nanosekunden-Zeitauflösung als Routinegerät aufzubauen und es zu charakterisieren. Dazu wurden alle Teile des Geräts auf ihre Funktion hin überprüft und die optimalen Parameter für die unterschiedlichen Meßmethoden bestimmt. Darüber hinaus wurde eine ultraschnelle Photodiode als Signalgeben für den Oszilloskoptrigger dem Aufbau hinzugefügt, um eine erhöhte Signalstabilität zu garantieren.

 Weiters sollten bereits gut charakterisierte organische Halbleitermaterialen vermessen werden. Im Besonderen wurden zwei halbleitende Polymere und zwei Fullerene, die bei der Produktion von organischen Solarzellen zu Anwendung kommen, untersucht. Von den Polymeren wurde das Lumineszenzspektrum gemessen sowie das Lumineszenz - Auslöschungsverhalten in der Mischung mit einem der Fullerene. Von beiden Fullerenen wurden die photoinduzierten Triplett-Absorptionsspektren gemessen.

Des Weiteren wurde eine Studie zur Lumineszenzauslöschung von Zinkphthalocyanin und einem neuartigen löslichen Fullerenderivat durchgeführt, um den Einfluss der koordinativen Bindung, welche sich zwischen den beiden ausbildet, zu untersuchen.

Abstract

The aim of this work was to setup the recently purchased nanosecond transient spectrometer for routine use. Therefore all important parts of the system were characterized and their functionality was tested. Furthermore the optimal parameters for the different measuring methods were determined. An ultrafast photodiode was introduced to assure an optimal temporal stability of the signal.

In addition, already well characterized organic semiconducting materials have been measured as references for future studies. Two different semiconducting polymers and two fullerenes commonly applied in the fabrication of organic solar cells were analyzed. The photoluminescence spectra of the polymers were measured as well as the luminescence quenching upon addition of one of the fullerenes. Measurements of the photoinduced triplet absorption spectra of the fullerenes were performed.

Furthermore a quenching study of zinc-phthalocyanine together with a new soluble fullerene derivative was performed in order to see the influence of a coordinative bond formed between these two molecules.

Table of contents

Acknowledgment

Chapter 1

1 Introduction

1.1. Optical Transitions in Molecules

In general molecules can exist in a non excited state and in an excited state. The transition between these two states can be instigated by an oscillating electric field. In the case of optical spectroscopy this field is provided by illumination. The probability of the transition between two states in a quantum mechanical system can be calculated as follows:

$$\mu_{fi} = \int \Psi_f \mu \Psi_i dV \tag{1.1}$$

$\mu_{fi:}$ transition dipole moment

$\Psi_f:$ wave function of the final state

$\Psi_i:$ wave function of the initial state

$\mu:$ operator, $\mu = -e\mathbf{r}$

Formula 1.1 expresses the probability of the molecule to be excited from the initial state to the final state through interaction with an electric field.

If the initial state is the ground state of the molecule the transition is then called absorption and if the initial state is the excited state the transition is called emission.

The definition of the transition dipole moment refers to one molecule. In the case of absorption, for a larger number of molecules this has to be extrapolated. The correlation between μ_{fi} and the integrated absorption coefficient $\mathcal{A}$ is given by:

$$\mathcal{A} = \frac{2\pi^2 \nu_{fi}}{3\varepsilon_0 ch} L |\mu_{fi}|^2 \tag{1.2}$$

$\mathcal{A}:$ integrated absorption coefficient

$L:$ Loschmidt number

$\nu_{fi}:$ frequency

$c:$ speed of light

$\varepsilon_0:$ vacuum permitivity

$h:$ Planck's constant

This integrated absorption coefficient corresponds to the intensity decrease in an absorption measurement via the Beer-Lambert law:

$$I = I_0 e^{-\mathscr{A}cd} \tag{1.3}$$

This describes how the intensity, I, of the radiation that is transmitted through the sample decreases with increasing path length d. c is the concentration of the absorbing molecules. It must be noted that $\mathscr{A}$ is the absorbance in a spectral band, because the same transition in different molecules does not have to happen at exactly the same wavelength. In most absorption measurements the coefficient is determined monochromatically. The absorption coefficient is then called α and is connected to $\mathscr{A}$ via:

$$\mathscr{A} = \int \alpha d\upsilon \tag{1.4}$$

It is possible to define $\mathscr{A}$ via the dimensionless oscillator strength f:

$$f = \frac{4m_e c\varepsilon_0}{Le^2} \mathscr{A} \tag{1.5}$$

e: charge

m_e: mass of electron

Therefore it is connected with the transition dipole moment via:

$$f_{fi} = \frac{8\pi^2 m_e \upsilon_{fi}}{3e^2 h} \left|\mu_{fi}\right|^2 \tag{1.6}$$

[1,2]

1.2. Laser Flash Photolysis

In 1949 Porter and Norris introduced the Flash Photolysis technique [3]. It is used for the detection of transient species. These transient species can be excitations of atoms, molecules or fragments of molecules which have a lifetime of less than 1 ms. By other techniques these species can not be observed, because the observation time is too long. The steady state measurement of absorption or fluorescence spectra takes a least some seconds. Transient species exist for only a fraction of seconds and therefore of course the observation time is far too long.

Therefore the flash photolysis is used for the study of photochemical and photo physical properties of compounds under illumination.[3] If one wants to study the absorption characteristics of transient species the sample has to be excited first by a ground state absorption. The reason for that is that such species do not occur in undisturbed molecules.[4]
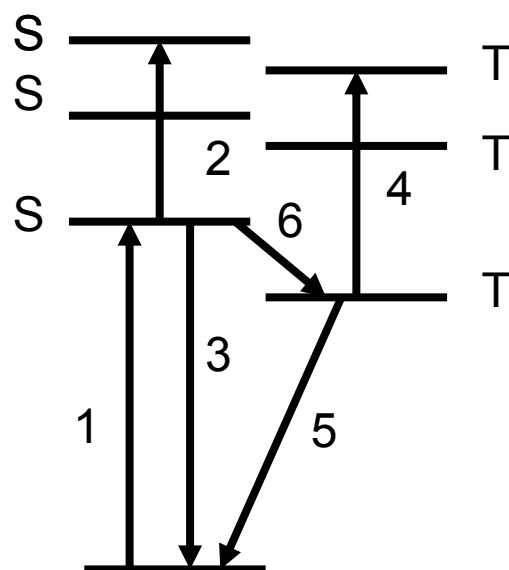
Figure 1. 1 Energy scheme 1: ground state absorption 2: excited state singlet – singlet absorption 3: fluorescence 4: excited state triplet – triplet absorption 5: phosphorescence 6: inter system crossing

An important information obtained by the flash photolysis is the lifetime of the excited state. This can be derived from the experiment directly without prior knowledge or calculation of additional rate coefficients. [6]

In order to generate these states in concentrations high enough to be observable one needs a powerful excitation source. This source is usually a laser.

Excited states can be divided into long living and short living states. The short living states usually have a lifetime in the range of picoseconds to 10's of nanoseconds while the long living states are in the range of 100's of nanoseconds to the time range of seconds. Short living excited states can be associated in most of the cases with singlet - singlet transition. The singlet excited state is often deactivated quite fast e.g. by fluorescence. For this reason there is not much time left for the excited species to undergo a further absorption into higher levels. The triplet state can usually only be deactivated by a spin forbidden process. Therefore it is a less likely transition to the singlet ground state. If a triplet state is once generated by an intersystem crossing they are long living and a spin allowed transition into higher triplet states is more likely.[2]

1.3. Measurement principle

In principle a laser flash photolysis setup is a single beam absorption spectrometer. But there is a difference: an additional pulsed laser excitation as a pump source.

The sample is in its ground state. It is excited by the pump source, which is in general a laser. The analysing light form the xenon lamp is passed through the sample at a right angle to the laser. Afterwards it is directed to the monochromator. This transmitted probe light is measured by a detector. The transmission properties of the sample before, during and after the laser pulse are converted by the detector into electrical signals. These signals are then measured by an oscilloscope.

Of course the flash photolysis needs a background level like all other absorption measurements. This background level allows the observation of changes in the transmission properties of the sample. A distinct difference to convential absorption measurements is the time scale of the measurement. Kinetics observed by the laser flash photolysis can be in the microsecond and nanosecond time scale. At those timescales the background photon flux of a tungsten lamp, or of an even more intense xenon lamp is not sufficient. For this reason one has to increase the background level. This is being achieved by operating the probing xenon lamp in a pulsed mode. This pulsed mode operation increases the photon flux a 100 times during the pulse. Therefore one can increase the signal to noise ratio for those time scales. [5] For the measurement of a triplet-triplet absorption this means that laser light pulse is used to create a high concentration of singlet excited molecules which undergo intersystem crossing to for the T_1 state. The flashlamp pulse of the Xe lamp provides the monitoring beam. Thus, as long as there is no laser pulse no triplet-triplet absorption will be monitored. Once the laser excites the sample the intensity of the transmitted probe light will go down due to the absorption of the triplet state. [6](Figure 1.2)
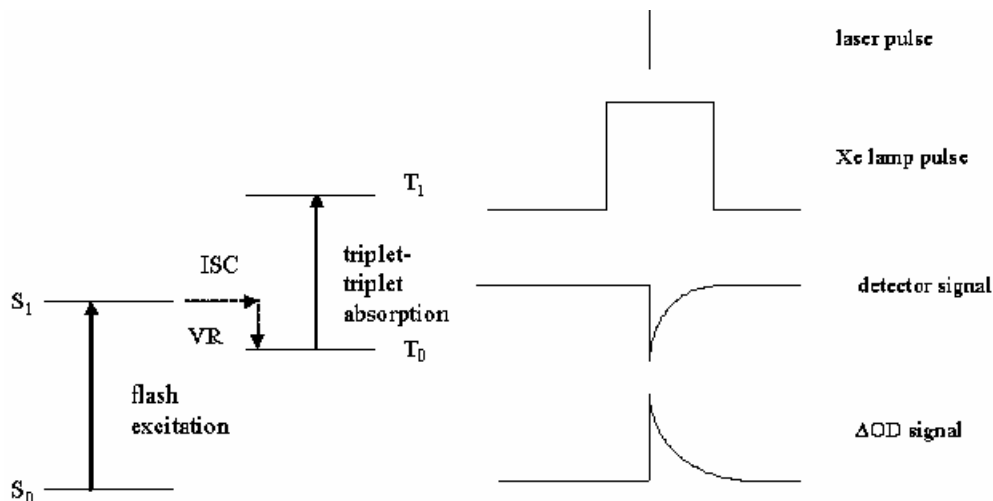
Figure 1. 2 Triplet-Triplet absorption created by the laser pulse and correlation of pulses and signal

1.4. The Δ OD

The flash photolysis spectrometer monitors the intensity (I_T) of the transmitted probe light through the sample during, shortly before and after the intense laser pulse. This laser pulse converts a substantial amount of ground state molecules into an excited state. Because of the change of transmission one can calculate the change in absorption in units of optical density, Δ OD:

$$\Delta OD(t,\lambda) = \log \frac{I_{100}}{I_T(t,\lambda)} \tag{1.7}$$

I_{100} :   light level measured through the sample before laser pulse

In general terms neglecting the singlet – singlet transition, the Δ OD can be summarised as follows

$$\Delta OD(t,\lambda) = \varepsilon_T(\lambda)c_T(t)d - \Phi(\lambda)c_S(t) \tag{1.8}$$

ε_T: extinction of the transient
c_T: concentration of triplet state
c_S: concentration of singlet state
d: effective path length of probe beam

9

Φ: fluorescence spectrum of the sample

In the spectral region where no fluorescence takes place, Φ is equal to zero. The true triplet – triplet features are therefore revealed by the observable Δ OD:

$$\Delta OD(t,\lambda) = \varepsilon_T(\lambda)c_T(t)d \qquad (1.9)$$

According to formula 1.3 the Δ OD is positive and decays as shown in Figure 1. 3 and Figure 1.2

Figure 1. 3 Δ OD decay

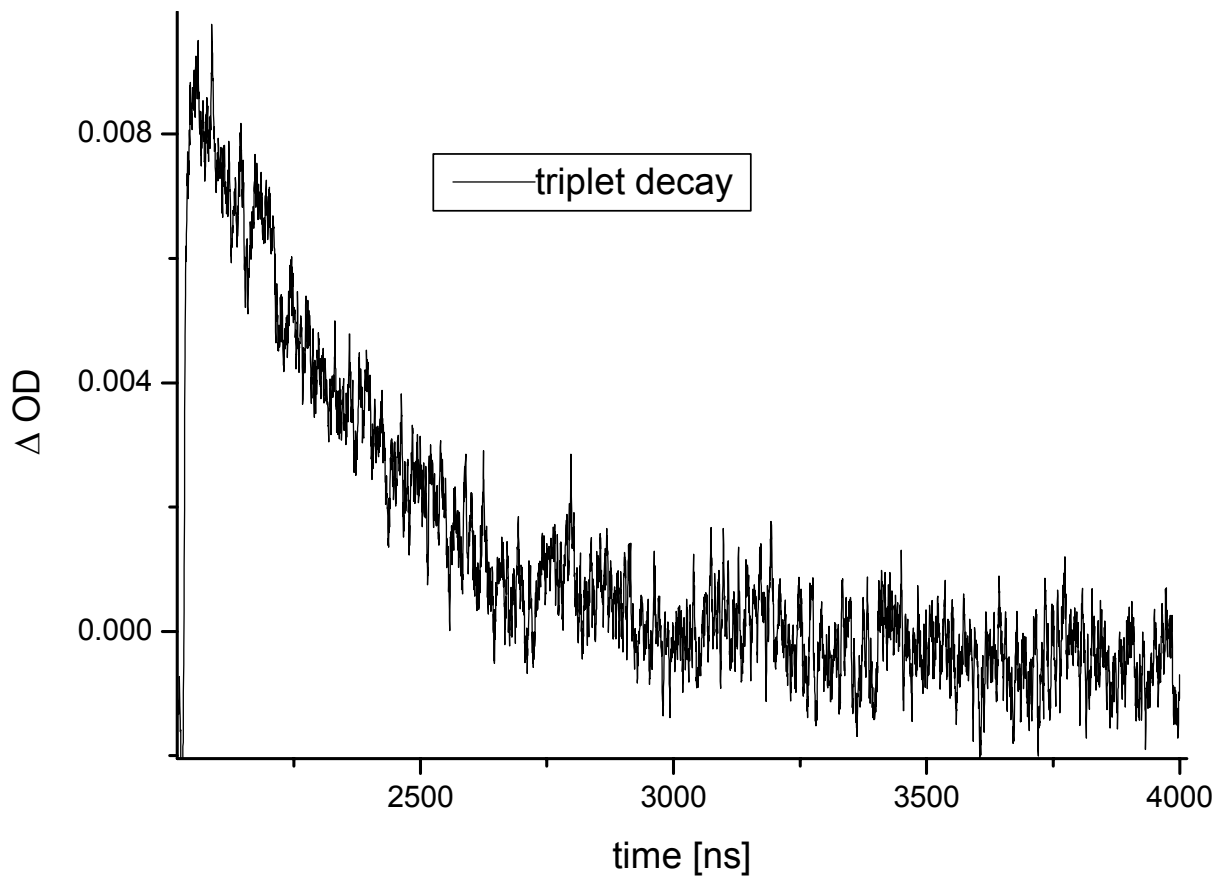Spectral regions with fluorescence results in a negative Δ OD. The decay times are much shorter because it is associated with short living singlet states. Fluorescence produces an

additional light at the probe wavelength and has therefore an influence on the measured transmission. [5]

In general an experimental measurement of the absorption intensity is provided by the Beer – Lambert law:

$$I = I_0 e^{-\alpha c d} \tag{1.10}$$

which describes how the intensity, I, of the radiation that is transmitted through the sample decreases with increasing path length d. α is the absorption coefficient. Dividing α by ln10 leads to the extinction coefficient.

For measuring a triplet-triplet absorption is equal to ε is equal to ε_T and c has to be replaced by c_T.

The product $\varepsilon c d = A = \log(I_0/I)$ is called the absorbance of the sample or optical density. [1]

1.5. Kinetics

1.5.1. The Jablonski diagram
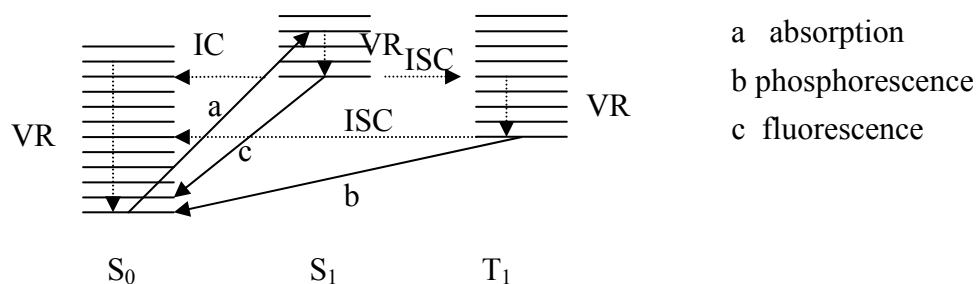
Figure 1. 4 The Jablonski diagram

All types of transitions can be summarized in a Jablonski diagram, which is in general a simplified energy diagram where the transitions are indicated by arrows. In Figure 1. 4. an example of such a diagram is provided. The vibrational levels of the ground state are shown on the left hand side (S_0) and those of the S_1 and T_1 state on the right hand side. Radiative transitions are indicated by solid arrows and non radiative transitions are indicated by dashed arrows.

11

The absorption is shown to occur from the S_0 (vibrational groundstate) state to some excited vibrational S_1 state. Through collision with solvent molecules vibrational relaxation (VR) to the vibration ground state of S_1 occurs extremely fast. From this level all subsequent processes occur. These processes may include fluorescence, internal conversion (IC) or intersystem crossing to the T_1 state. If the T_1 state is formed it may decay by emitting phosphorescent light, undergo a reversed inter system crossing or further absorption of radiation to excite a T_2 state.

Organic photochemistry normally deals with the properties and the reactivities of the S_1 and the T_1 state of organic molecules. If the S_2 state is formed, a rapid internal conversion to the S_1 state usually follows, so S_2 does not have to be taken into account. [6]

1.5.2. Radiative lifetimes

1.5.2.1. First order decay

If only radiative processes are considered a situation can be imagined where a certain concentration of an electronically excited molecule $[M^*]$ is formed. It decays to zero as a function of time due to emission of radiation:

$$M^* = M + h\nu' \tag{1.11}$$

In the formula shown in 1.4 hυ' is a lower or equal energy compared to the one, which was originally absorbed by the ground state molecule M. The spontaneous emission is a random process and such random processes follow first order kinetics:

$$-\frac{d}{dt}[M^*] = k_r^0[M^*] \tag{1.12}$$

where k_r^0 is the rate coefficient. This characterizes the rate of the spontaneous emission process and it is determined by the nature and the properties of the emitting state. The subscript r stands for radiative and it can be replaced by f (fluorescence) or p for (phosphorescence)

Integration of 1.5 leads to

$$[M^*] = [M^*]_0 e^{-k_r^0 t} \tag{1.13}$$

The concentration of M^* decays therefore exponentially towards zero from a initial state concentration $[M^*]_0$ at the time 0.

In photochemistry the rate of an emission process is usually characterized by the lifetime. τ_r^0 (natural lifetime) is defined as the reciprocal of the radiative rate.

$$\tau_r^0 = \frac{1}{k_r^0} \qquad (1.14)$$

The radiative rate has the units of s^{-1} and therefore the lifetime has units of s.

Under the circumstances of the flash photolysis the measured rate coefficient k_r can not be identified as k_r^0, because additional processes might contribute to the decay.

The fluorescence of the S_1 state of M might be in direct competition to the IC (to give a vibrationally excited S_0 state) and ISC (to T_1). The rate of the decay of $[M^*]$ is then given by

$$-\frac{d}{dt}[M^*] = k_f^0[M^*] + k_{ISC}[M^*] + k_{IC}[M^*] \qquad (1.15)$$

k_f^0:   natural fluorescence rate coefficient

k_{ISC}:   rate coefficient for ISC

k_{IC}:   rate coefficient for IC

The decay of $[M^*]$ is still first order, but now with a rate coefficient of k_f:

$$[M^*] = [M^*]_0 e^{-k_f t} \qquad (1.16)$$

with

$$k_f = k_f^0 + k_{ISC} + k_{IC} \qquad (1.17)$$

This means that the rate coefficient k_f includes all of the possible decay channels for $[M^*]$. This can be summarized as

$$k_f = \sum k_i \qquad (1.18)$$

If i = f the superscript 0 is added.

The measured fluorescence lifetime is therefore:

$$\tau_f = \frac{1}{k_f} = \frac{1}{\sum k_i} \tag{1.19}$$

[6]

Formula 1.9 can be also given in a more general form as

$$c(t) = c_0 e^{-k_1 t} \tag{1.20}$$

where $[M^*]$ is replaced by the general concentration at the time t. c_0 is the concentration at t=0 and the k_f is replaced by a general first order decay rate constant k_1.

By including 1.12 to this formula one ends up with :

$$c(t) = c_0 e^{-\frac{t}{\tau_1}} \tag{1.21}$$

[5]

In the flash photolysis emission measurements can also be done. In this case there is no flash lamp pulse, only the laser is exciting the sample and the light from the sample is detected. From the traces obtained by these measurements the lifetime can be directly calculated (without calculating the ΔOD first) by fitting the trace with formula 1.14, as can be seen in Figure 1. 5
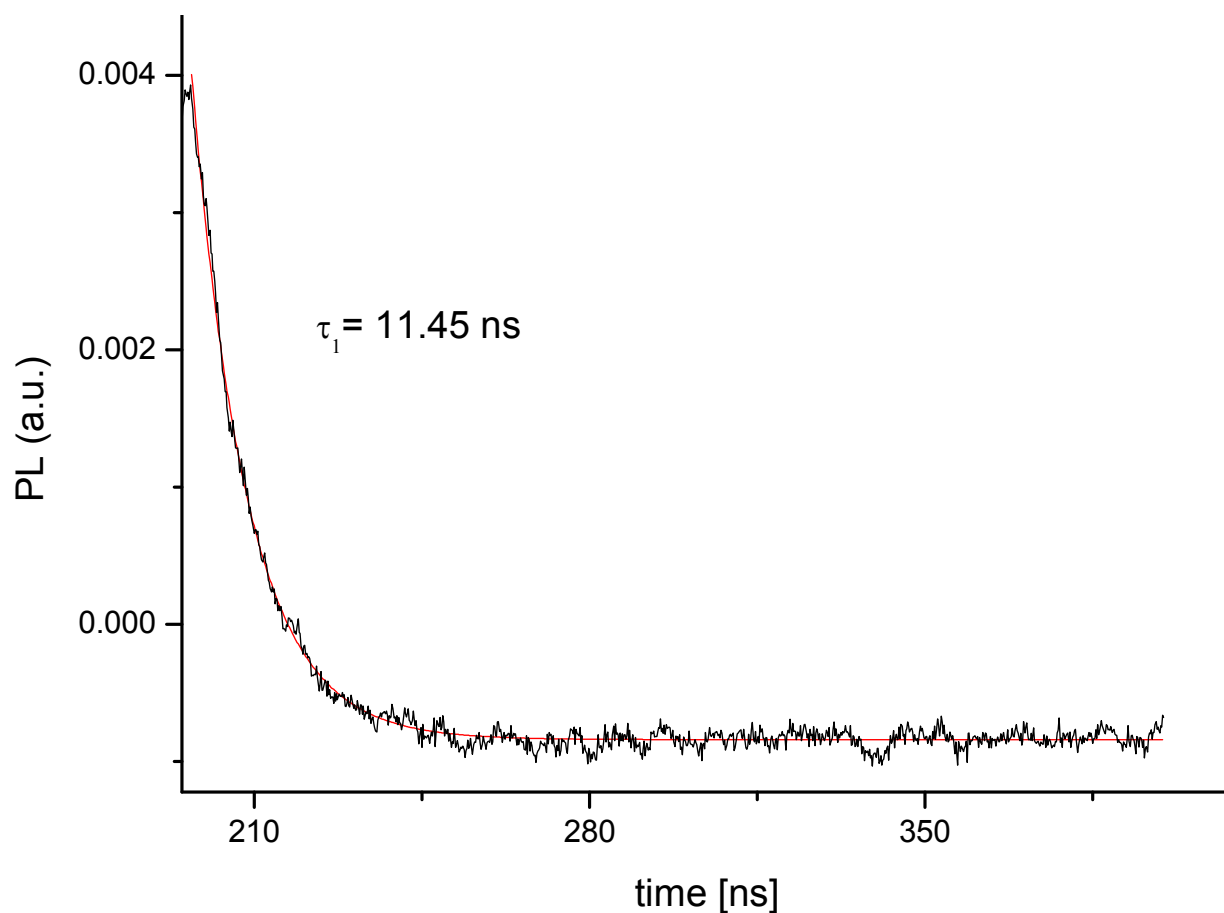
Figure 1. 5 Emission trace fitted with formula 1.14 and the calculated lifetime

In the case of absorption measurements the initial burst of laser light is used to create a high concentration of S_1 molecules which undergo ISC and VR to the T_1. The lamp provides a monitoring beam which wavelength is selected to match with the triplet – triplet absorption feature in the T_1 spectrum (Figure 1. 6) [6]

Figure 1. 6 Schematic diagram for the absorption in the flash photolysis

In this case the Δ OD should be calculated first and the lifetime can be extracted from the trace by exponential fits according to

$$\Delta OD = \Delta OD_0 e^{-\frac{t}{\tau_1}}$$ (1.22)

where ΔOD_0 is the initial difference absorbance. [5]

1.5.2.2. Pseudo first order decays

If the excited state is being quenched by a second species, i.e. molecular oxygen, an enhanced rate of decay is observed relative to monomolecular decay.

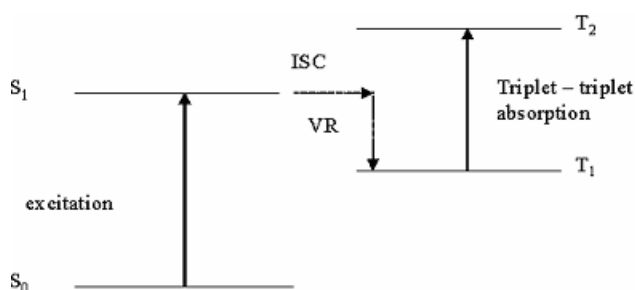$$-\frac{d}{dt}[M^*] = k_1[M^*] + k_q[M^*][O_2]$$ (1.23)

In general the ground state oxygen concentration is around 10^{-3} to 10^{-4} M and is therefore much grater than the one of the triplet state, which is usually around 10^{-6} to 10^{-7} M. For this reason a pseudo first order kinetics are observed. Thus the decay follows the same law as given in 1.14 and 1.15 but the rate constant now is k_2:

$$k_2 = k_1 + k_q[O_2]$$ (1.24)

The observed rate constant is k_2, which is increased in comparison to k_1, i.e. a faster decay time.

By measuring the fluorescence in the presence of a quencher [Q] $\frac{k_q}{k_f}$ can be determined by the Stern – Volmer plot, where $\frac{I_f^0}{I_f}$ is plotted against [Q] (Figure 1. 7):

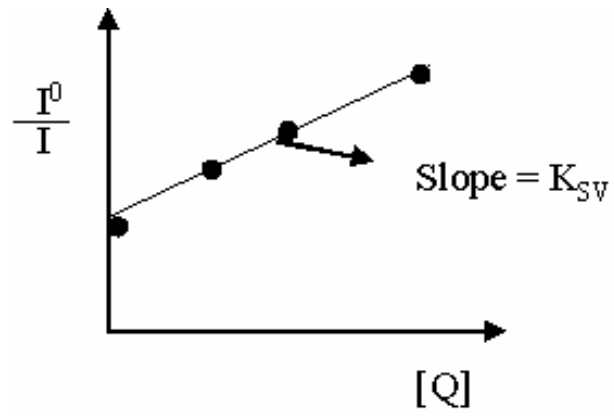$$\frac{I_f^0}{I_f} = 1 + \frac{k_q[Q]}{k_f}$$ (1.25)

Figure 1. 7 A typical Stern-Volmer Plot

In the Stern – Volmer plot the slope of the curve is the Stern – Volmer constant K_{SV}:

$$K_{SV} = \frac{k_q}{k_F} = \tau_F k_q \qquad (1.26)$$

This means that the higher the constant the more efficient is the quenching.[6]

Chapter 2

2 Experimental

2.1. The Experimental Apparatus

The following chapter will deal with the setup of the LP920. For further details the manual can be consulted. [5]

A picture of the LP920 system from Edinburgh Instruments can bee seen in Figure 2. 1 and a schematic view of the system is shown in Figure 2. 2 The samples were solutions of the investigated materials in a 1 cm x 1 cm cuvette.

2.1.1. Probe light source Xe920

The probe light source is a 450 W ozone free Xe arc lamp, which produces a continuouse spectrum between 150 to 2600 nm. It has intense lines between 800 and 1000 nm. This lamp can be used in a continuous and in a pulsed mode up to 10 Hz.

2.1.2. Pulser Unit XP920

This unit works in combination with the Xe920 and the power supply and provides a good rectangular pulse with fast rising and falling edges. It can provide pulse widths up to 10 ms in a power range from 50 to 300 A. This 300 A is a maximum value of lamp power set by the company to avoid damages of the lamp during operation. The value results from a combination of voltage supplied to the lamp, repetition rate, pulse current and pulse width:

$$P = 60ITf \tag{2.1}$$

where P is the power, I is the current, T the pulse width and f the frequency. Pulse current and width can be adjusted by the user. 60 V is the constant value of the lamp voltage during pulsing.

The XP920 can produce short period high current pulses allowing the Xe lamp to flash. The typical optical profile of a pulse generated with the pulser unit can be seen in Figure 2. 3
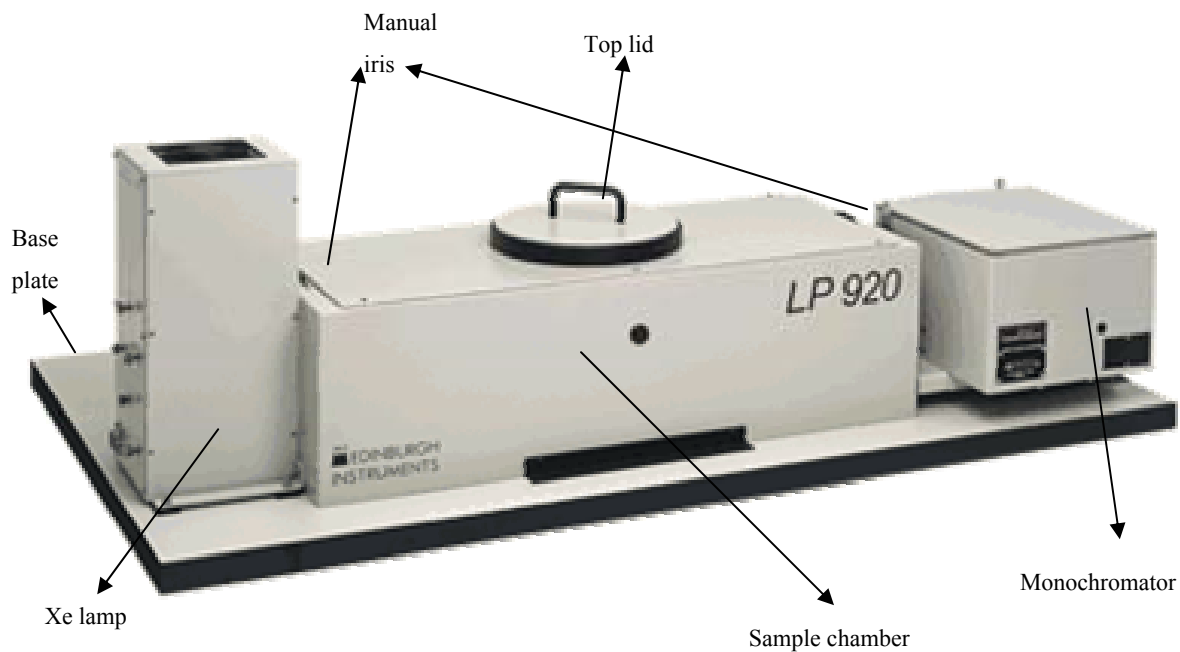
Figure 2. 1 Picture of the LP920 Laser Flash Photolysis Spectrometer from Edinburgh
Instruments
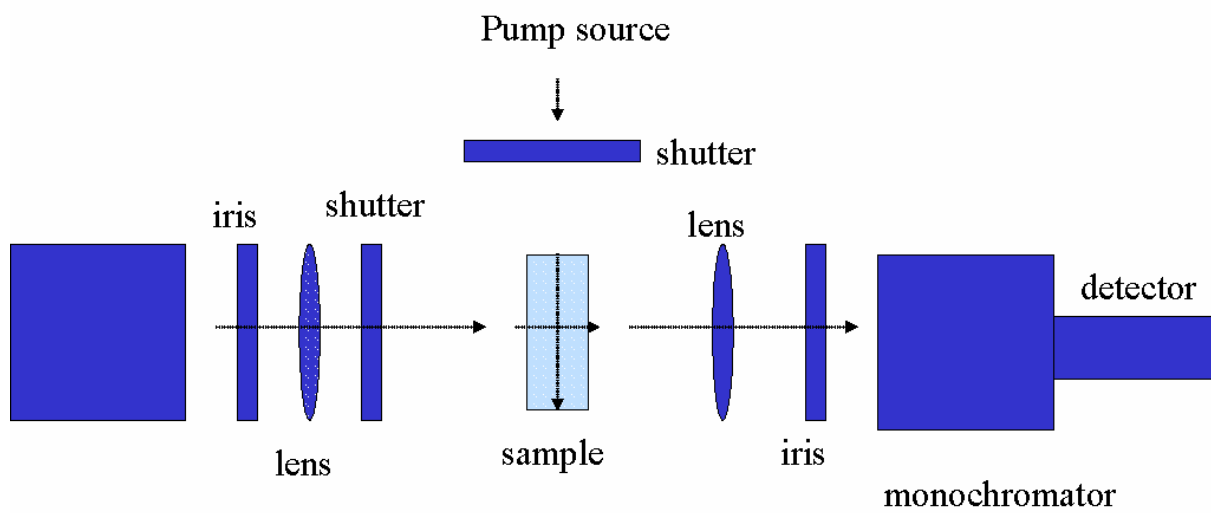
Figure 2. 2 Schematic Scheme of the Flash Photolysis Spectrometer
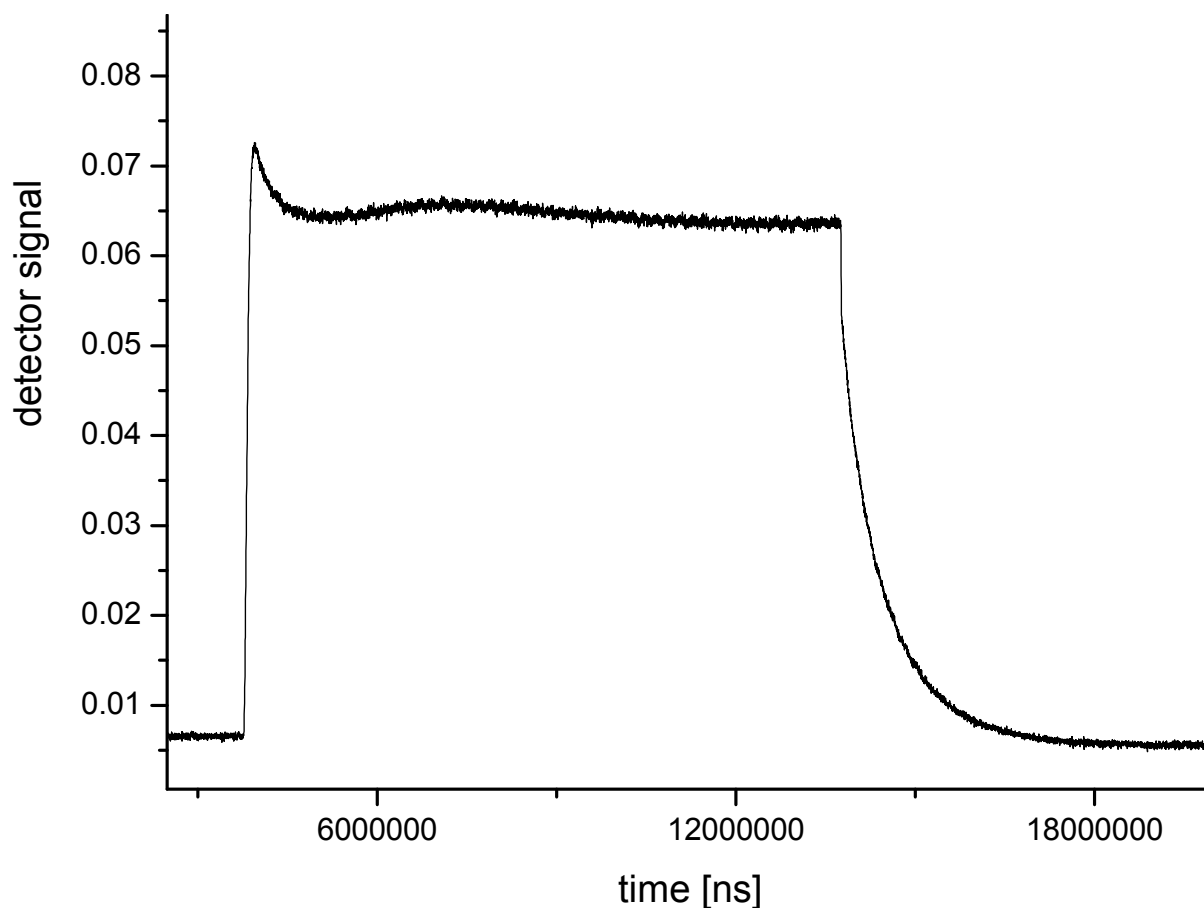
Figure 2. 3 Typical optical pulse profile generated with the pulser unit XP920

The falling and the rising edge of the trigger control the width of the pulse and the pulse height of the trigger determines the amplitude of the current pulse.

The pulse width can be adjusted from 0.2 ms to 10 ms.

2.1.3. Spectrometer Controller LP920

This controller is the central timing unit for all components of the spectrometer. In addition, it is the bias supply for most of the components of the spectrometer. It also comprises the interface with the L900 software. Furthermore it provides the control to the pulse of the lamp, laser flashlamp and laser Q-switch and operates the probe and laser shutters. The control of the positioning of the monochromator and the voltage supply to the PMT detector is also done with the controller unit.

2.1.4. Monochromator TMS300

The monochromator in the system is a symmetrical Czerny-Turner monochromator. Its design utilises all – reflective optics to maintain a high resolution over the entire spectral range. It has a focal length of 300 mm and a constant aperture of $\dfrac{F}{4.1}$.

The core is a plane reflection grating, which disperses the incident light via vertical grooves in the surface. For the acquisition of traces at a single wavelength, the monochromator is fitted with a 1800 lines mm^{-1} grating which is blazed at 500 nm and covers a wavelength range from 300 to 900 nm. For measurements in the near infrared regime the grating has 600 lines mm^{-1}, blazed at 1000 nm.

The maximum resolution for the 1800 lines mm^{-1} grating is 0.05 nm and for the NIR grating it is 0.15 nm

The monochromator incorporates a computer controlled swing mirror at the exit port, which allows a fast selection of the detector. Both the entrance and the exit ports are fitted with computer controllable slits which control the spectral bandwidth of the signal to be measured. The setting of the slits is calibrated in wavelength units and the software automatically scales the settings dependent on the grating in use.

2.1.5. PMT Detector (SP300)

The detector is a red sensitive photomultiplier (Hamamatsu R928) and covers a wavelength range from 185 to around 850 nm (Figure 2. 4).

There are two modes of the detector: The fast amplifier circuit has a rise time smaller than 1 ns for a output impedance of 50 Ω. This design is suitable for measurements of transients up to 100 μs. For measurements at larger time scales there is a slow version of the detector which gives a better signal to noise ratio. This circuit has a rise time of 1 μs and a 1 k Ω output impedance.

2.1.6. NIR Detector

This detector is a two stage thermo electrical InGaAs PIN photodiode (Hamamatsu G5852-21). It covers a wavelength range from 850 to 2100 nm, as can be seen in Figure 2. 5
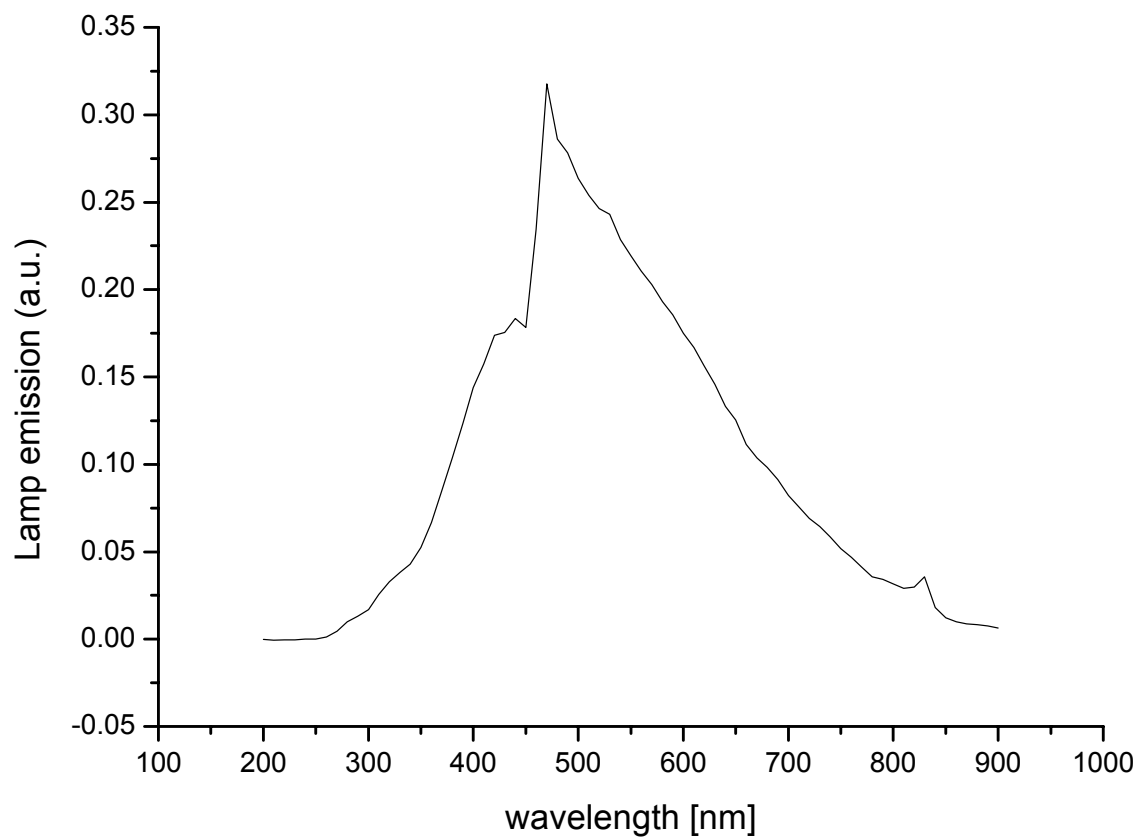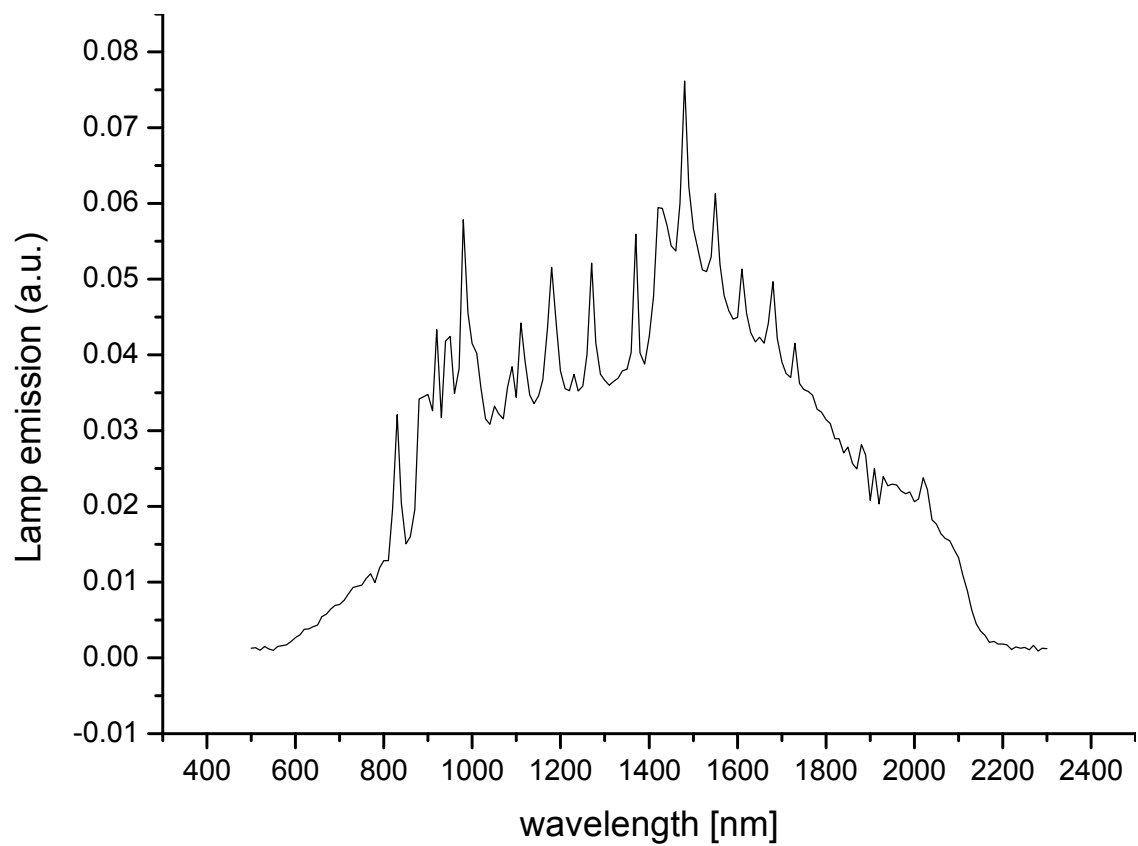
Figure 2. 4 Lamp signal for the PMT detector

Figure 2. 5 Lamp signal for the NIR detector

22

2.1.7. Oscilloscope (TDS3012B)

The signals coming from one of the two detectors are recorded by an oscilloscope (Tektronix TDS3012B). It is used as a real time transient digitiser. For routine operations of the spectrometer the oscilloscope can be operated with the spectrometer software. For providing a fast data transfer, the computer is connected via Ethernet to the oscilloscope.

For triggering the oscilloscope an ultra fast photodiode (Newport 818-BB-20) is used because that this way of triggering works better than using the trigger signal from the laser, as this rather unstable. Therefore a small glass plate was mounted in front of the laser, so that a small part of the laser beam is directed to the photodiode.

2.1.8. Sample Compartment

This is a large light tight box where the access is given by the removal and replacement of a circular lid in the centre of the sample chamber (Figure 2. 6 and Figure 2. 2). The detectors have an interlock with the lid, which mean removal of the lid leads to closing of a detector shutter located at the entrance of the monochromator to protect the detector units from ambient light.

The sample chamber has the following components

- Focusing lenses

  One is at the output of the Xe lamp and the second one is at the entrance of the monochromator. The focusing lens on the output of the Xe lamp produces an image of the lamp arc at the sample position (magnification 2.5). The hot spot of the xenon lamp on the image is around 3 mm in diameter. The image of the light that has passed the sample into the monochromator is inverse symmetric to the focusing from the lamp.

- Electronic shutters

  In the sample chamber there are two high speed shutters. The probe shutter is located in front of the sample. It should first protects the sample from photobleaching and photodegradation which is due to long exposure by the xenon lamp in the time where it is not necessarily needed for the measurement and second it blocks the probe light for emission measurements (or emission background measurements).

  The second shutter is the laser shutter and this blocks the laser shots for probe background measurements.

Both of the shutters are fully synchronized within the measurement sequence. In addition both of them can be controlled via the software.

- Irises

The system incorporates two manual irises both of them located in the proximity of the focusing lenses. They are primarily used for light attenuation. There is a third iris directly after the sample holder.
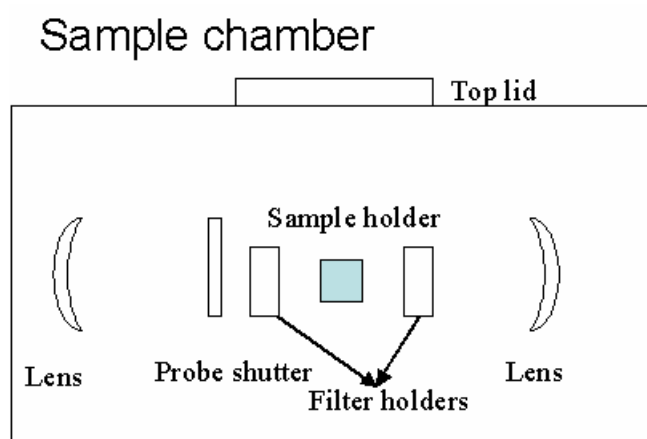

Figure 2. 6 Side view of the sample chamber

2.1.9. Sample Holder

The sample holder has a cross beam configuration where the pump laser beam and the probe beam are perpendicular and intersecting in the sample volume. The laser beam passes the sample centrally and is dumped on the sample chamber wall. The laser beam must be adjusted in height so that the same sample volume probed by the probe beam is excited most.
At the beam output there is an adjustable iris which allows the control of unwanted scattering or fluorescence. For absorption measurements, the iris is closed to approx. 3 mm diameter , which means closing it for about ¾.
For emission measurements the iris is wide open.

2.1.10.   Laser

The laser used with the system is a Coherent Infinity ^{TM} 40-100 Nd:YAG laser. It simultaneously produces a 3 ns laser pulse at 532 and 355 nm. To lead the laser light into the spectrometer Nd:YAG dielectric mirrors were used, one for each wavelength (Thorlabs NB1-H08 and NB1-H12)

2.1.11.   Timing

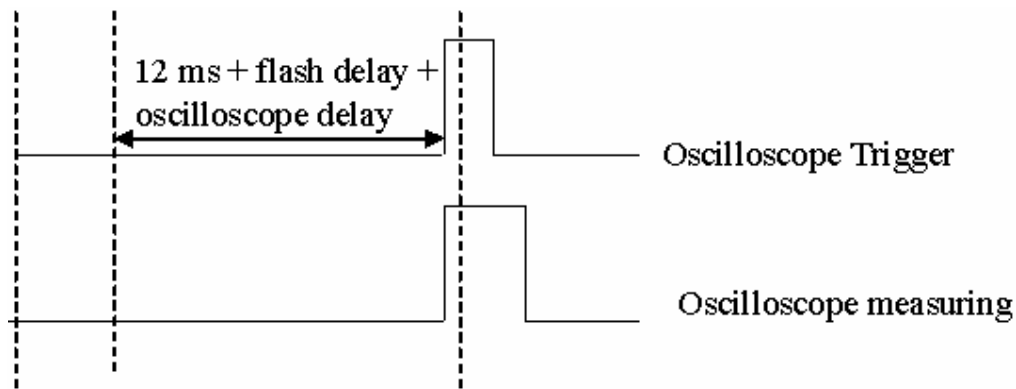A typical timing diagram can be seen in Figure 2. 7
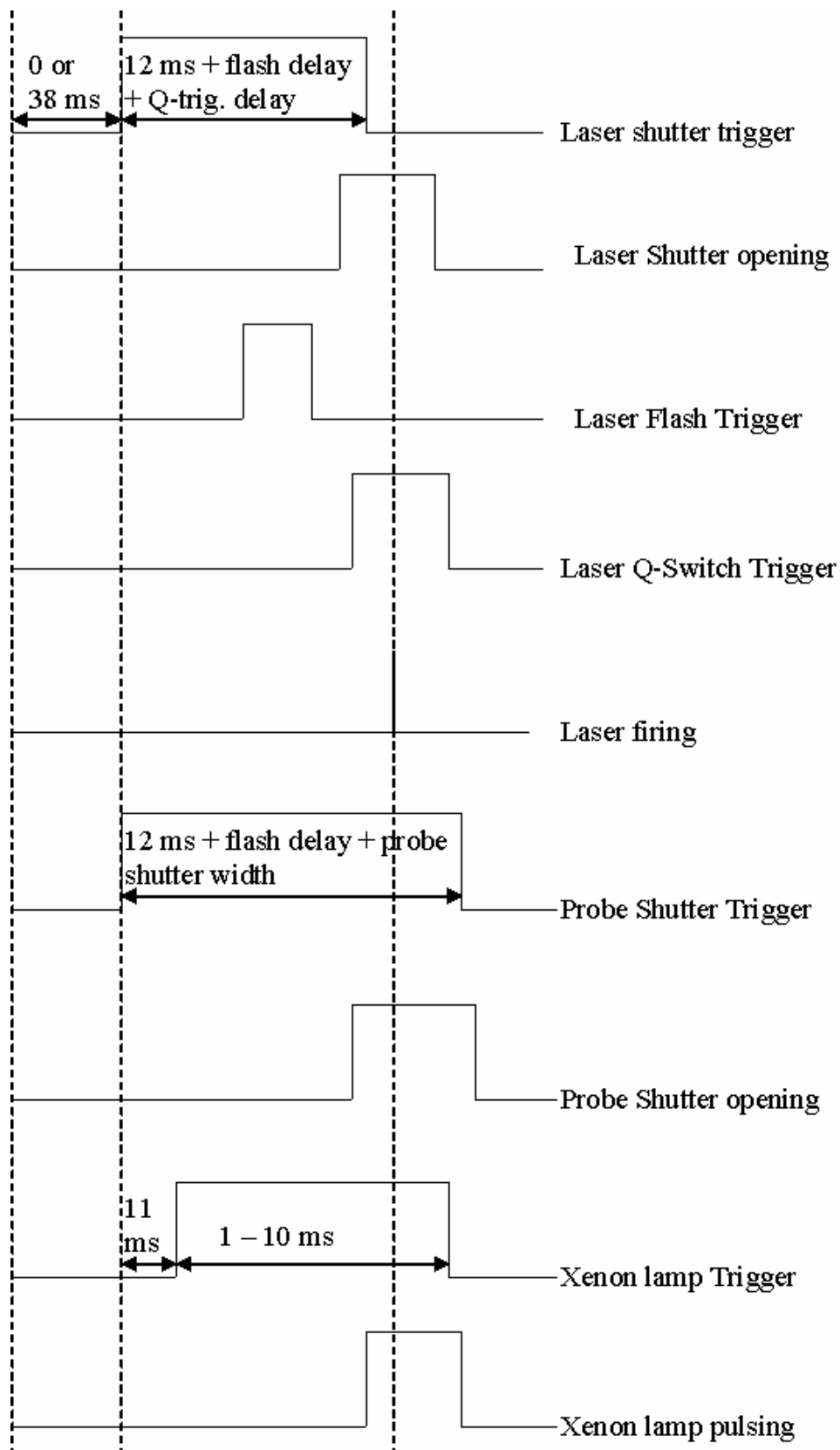
Figure 2. 7 Timing diagram

2.2. Software Description

All of the LP920 system components are controlled by the software of the instrument. In this section a short overview of the different parts of the software is in this section.

2.2.1. Laser Setup

It is possible to store 3 different laser configurations, called laser modes. In this case two different modes are used: a 1 Hz mode and a 10 Hz mode. The different settings can be designed by the user for specific requirements.

In general the flashlamp trigger initializes the pumping of the laser cavity. An ocusto optical modulating suppresses the lasing until the Q-switch trigger is applied. A laser pulse only occurs when both, flashlamp and Q-switch trigger are active.

The flashlamp delay enables to shift the flashlamp trigger of the laser in respect the xenon lamp pulse. This is done to be able to measure in the constant part of the Xe lamp profile. The additional Q-switch delay determines the interval between the laser flashlamp trigger and the laser Q-switch trigger.

The flashlamp pulse width is the width of the TTL pulse supplied by the controller to flash the laser head pump. The flashlamp pulse polarity allows the selection of the positive and negative slope of the TLL pulse sent by the controller to trigger the laser flashlamp. The repetition rate of the laser Q-switch (Q-trigger frequency) can either be set to the laser flashlamp frequency or to the LP920 acquisition frequency. The Q-switch pulse width determines the width of the TLL pulse to flash the laser Q-switch. The polarity of the TLL pulse allows the selection of the positive and negative slope of this TLL pulse.

The settings are adapted to the light sources used in our setup and have the following values:

Laser flashlamp delay	5000 μs
Additional Q-switch delay	258 μs
Flashlamp pulse width	10 μs
Flashlamp pulse polarity	- ve
Q-trigger frequency	LP920
Q-trigger pulse width	50 μs
Q-trigger polarity	- ve

2.2.2. Detector Setup

It is possible to change some settings of the oscilloscope trigger: the pulse width, the delay and the polarity of the oscilloscope trigger. These settings are adapted to the oscilloscope used and have the following values.

Oscilloscope trigger pulse width	50 μs
Oscilloscope trigger delay	258 μs
Oscilloscope trigger polarity	- ve

2.2.3. Port Setup

This allows selecting the monochromator exit (port) which is used for the measurement and this determines which detector will be used. It is possible to change the settings for the different ports e.g. the grating for the detector.

2.2.4. Measurements

There exist two types of measurements: Kinetic emission and Kinetic absorption. For each of those two there are 3 different subtypes modes: The setup mode, where it is possible to optimize the conditions for the following measurement. The multiple mode can be used to acquire data and/or get a signal average over a predetermined number of laser shots. The third mode is the map mode. Here it is possible to acquire traces over a whole wavelength range and slice them afterwards into spectra by applying the data slicing option.

In all cases there is the option of choosing the time range and the voltage range for an optimization of the signal.

2.2.4.1. Kinetic Emission

In this mode of measurements it is possible to obtain one luminescence spectra and decays. In emission measurements the probe shutter is closed, so that no light from the Xe lamp is exciting the sample. For Kinetic emission measurements the iris, which is located directly after the sample holder should be opened wide, to increase the signal. In most of the cases it is very useful to have a filter in the filter holder (located also after the sample chamber) to get rid of the first and second harmonic of the laser beam, which can have an unwanted influence on the spectra. (Figure 2. 8). In the experiments a 530 nm and a 385 nm glass filter (Schott Glass, OG 550 and GG 385, 1 mm thickness) were used. In Figure 2.8 c is just the range around the second harmonic laser spike.
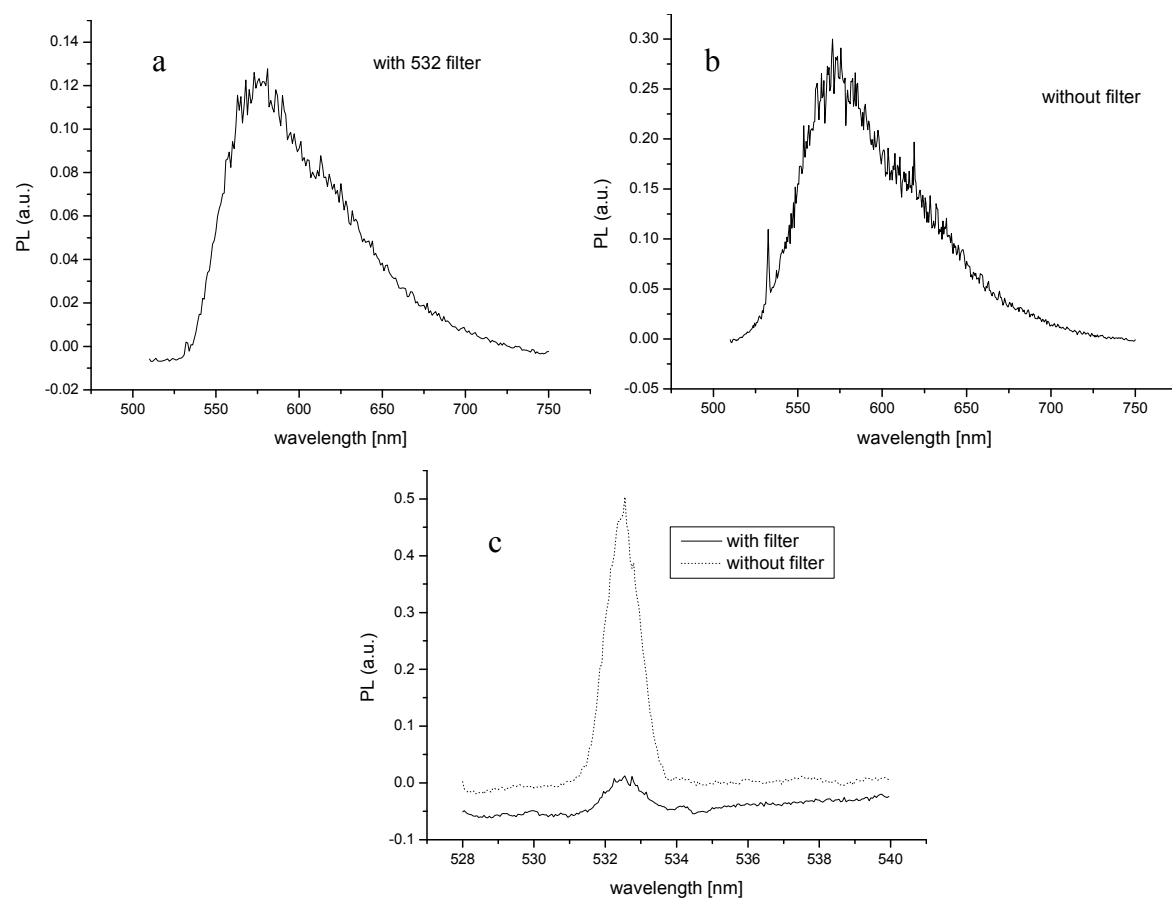
Figure 2. 8 Photoluminescence measurements of P3HT with and without the OG 550 filter

28

2.2.4.2.   Kinetic Absorption

This mode is used to collect transient absorption traces at both single wavelength and over a range of wavelength (map mode). After the measurement the traces are automatically converted into ΔOD values. The iris after the sample holder is closed to about ¾ for an optimal signal to noise ratio and to avoid saturation of the detectors by the intense Xe lamp background level.

In this mode there are some background corrections. Without any correction the ΔOD is calculated as described in formula 1.1.

The first type of correction is the probe background correction, this will compensate any drift in the 100 % background level caused by fluctuations in the probe light intensity. In this type, of measurement two traces will be collected for each wavelength. The first one will be the experimental decay, which means it contains laser and probe light. The second trace is a reference trace of the probe background level. In this case the laser light will be blocked by closing the laser shutter.

 The mathematical formula for the ΔOD is then:

$$\Delta OD(t) = \log \frac{I_{100}^{T}}{I_{100}^{PB}} + \log \frac{I_{PB}(t)}{I_{T}(t)} \tag{2.2}$$

where $I_T(t)$ is the time dependent intensity, $I_{PB}(t)$ the time dependent probe background and the indices 100 designate for the background level.

Sometimes the decay measurements may be influenced by a contribution from the sample fluorescence. To minimize this effect the fluorescence correction can be used. By doing this type of measurement there will also be two consecutive traces collected, the first one as described before and the reference trace is taken without the probe light, which means only the laser light is exciting the sample. Then the following mathematical formula will be used to calculate the ΔOD:

$$\Delta OD(t) = \log \left(\frac{I_{100}}{I_{T}(t) - I_{F}(t)} \right) \tag{2.3}$$

Both types of correction can be done in one measurement, the function applied for calculating the optical density is then as follows:

$$\Delta OD(t) = \log \frac{I_{100}^{T}}{I_{100}^{PB}} + \log \frac{I_{PB}(t)}{I_{T}(t) - I_{F}(t)} \tag{2.4}$$

[5]

2.2.5. Data Slicing

A very important part of the software is the data slicing option, with which it is possible to obtain time resolved spectra from of the collected traces. This option is only possible in the map mode.

It is possible to define one to 100 slices in the time domain. The detector signal value of all traces is taken at a single wavelength and plotted against the wavelength (Figure 2. 9-Figure 2. 11). In Figure 2. 9 the photoluminescence decay of KCl 006-4 [7] can be seen. In the 3 D plot (Figure 2. 10) it comes out quite clearly that applying the data slicing option result in a spectrum (Figure 2. 11). [5]
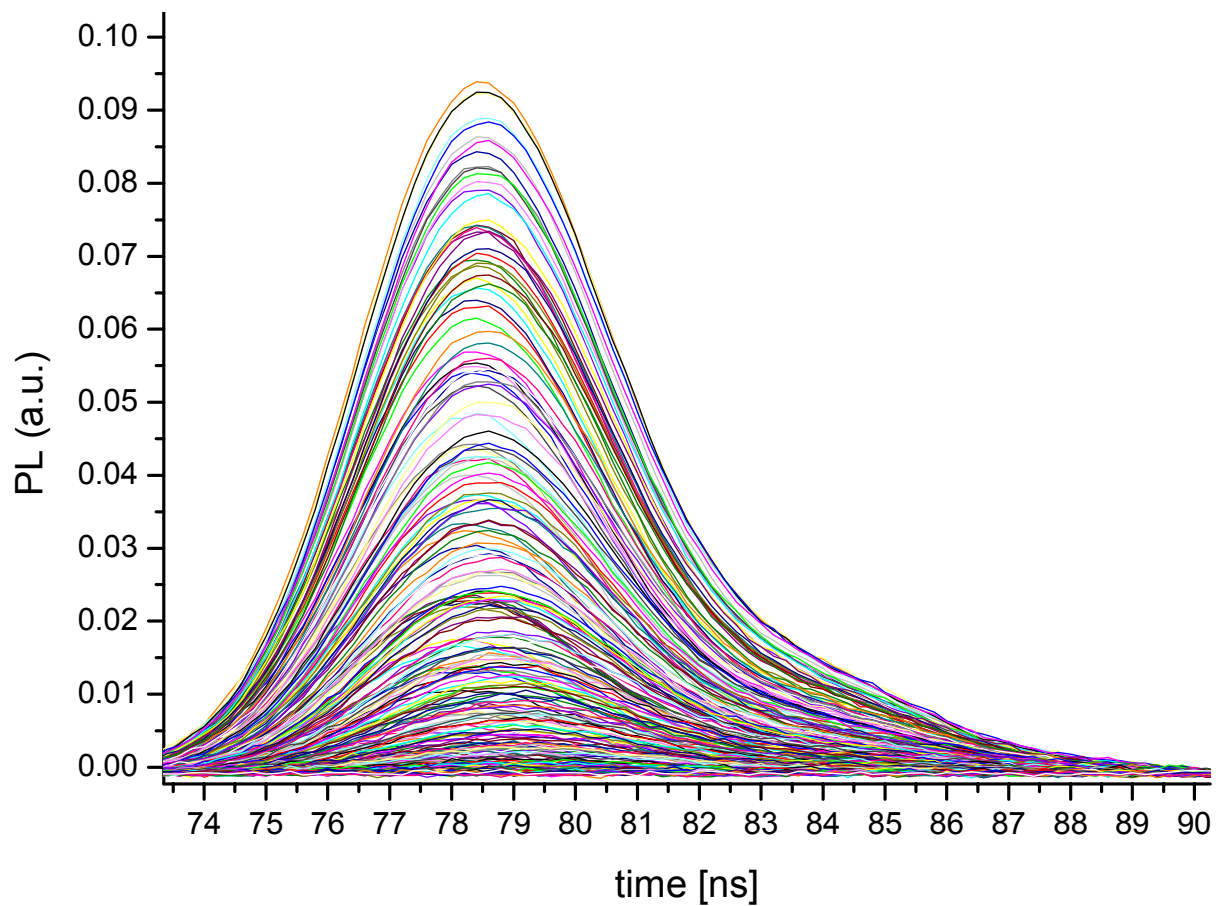

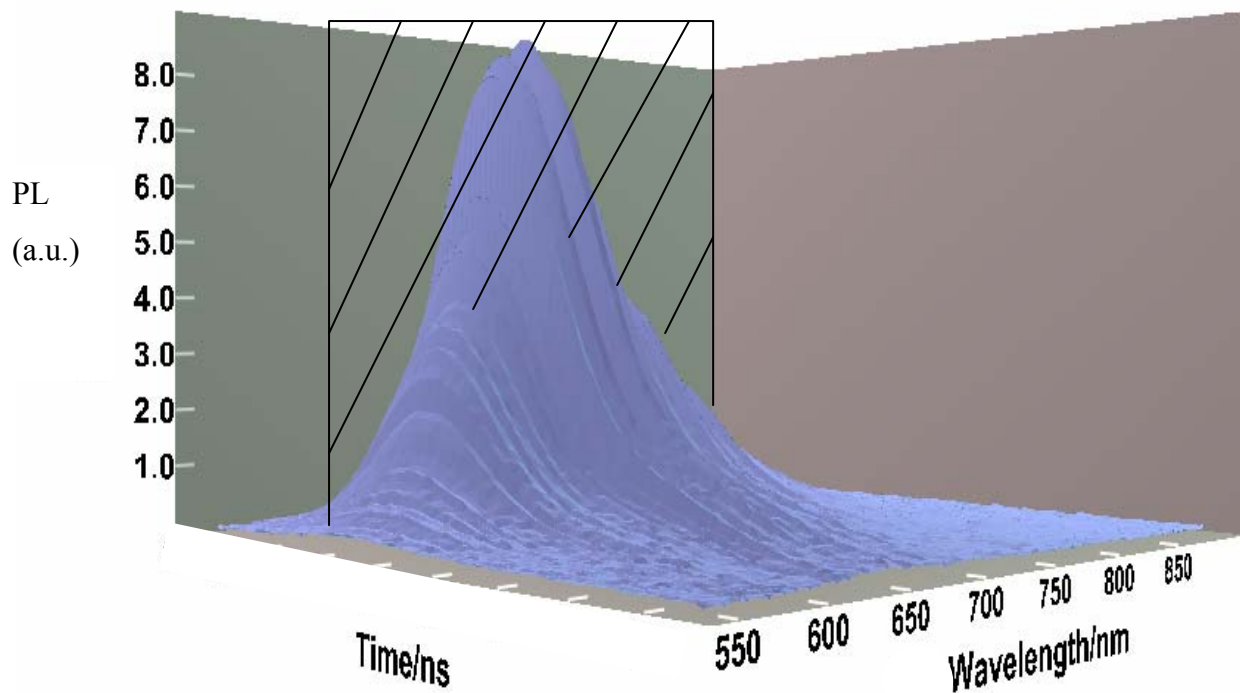
Figure 2. 9 Photoluminescence traces of KCl 006-4

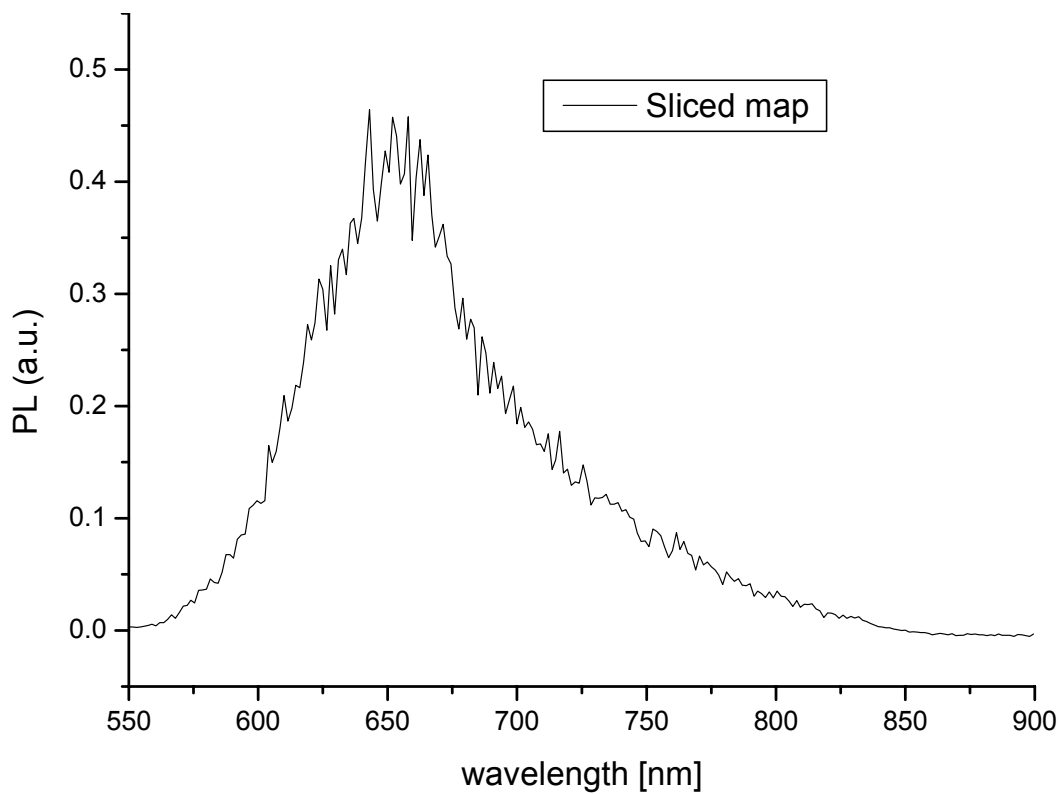Figure 2. 10 3 dimensional plot of Fig. 2.10

Figure 2. 11 Sliced spectrum resulting Fig. 2.10 and 2.11

2.3. Sample Preparation

All samples were measured in solutions. The concentration was chosen so that the optical density of the solution was around 1. It was found out that this value gives the best signal in the experiments. The solutions were filled in a 1cm x 1 cm x 4.5 cm quartz cuvette (Hellma QS 101) and then put into the sample holder. The cuvettes were in most cases sealed with parafilm to minimize evaporation losses and the diffusion of oxygen into the solution. The total amount of solution in the cuvettes was in most cases around 3 ml.

2.3.1. Materials

C_{60}

A 1.25×10^{-4} M solution of C_{60} in toluene was prepared. The solution was stirred over night in the glove box. Afterwards this solution was diluted to a concentration of 5×10^{-6} M inside the glovebox and sealed as proper as possible with parafilm.

Figure 2. 12 Chemical structure of C_{60}

MDMO – PPV

A solution containing 0.1 w% of poly-[2-(3,7-dimethyloctyloxy)-5-methyloxy]-para-phenylene-vinylene (MDMO – PPV) in chlorobenzene was prepared (Figure 2. 13). The polymer was handled inside the glovebox. The solution was stirred over night and then diluted to a 0.002 w% solution and sealed.
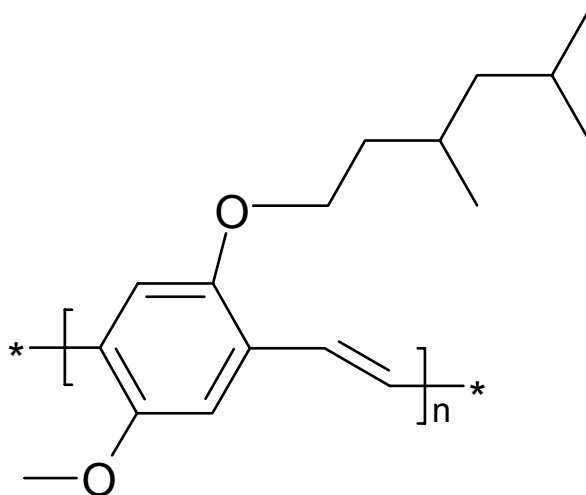
Figure 2. 13 Chemical structure of poly-[2-(3,7-dimethyloctyloxy)-5-methyloxy]-para-phenylene-vinylene; MDMO – PPV

P3HT

The P3HT solution contained 2 mg of regioregular poly(3-hexylthiophene-2,5-diyl) (Figure 2. 14) in 2 ml chloroform (0.1 w%). The material was handled inside the glovebox. The solution was stirred over 2 days. For the measurement the solution was diluted to a 0.002 w% solution and sealed with parafilm.
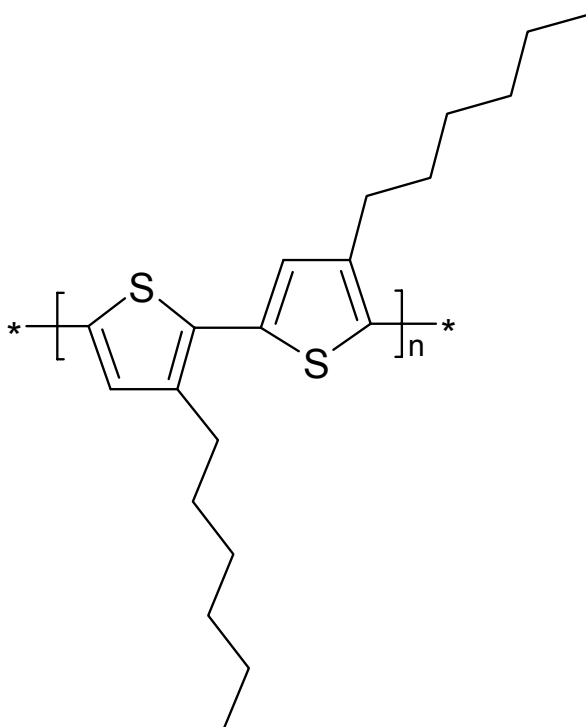

Figure 2. 14 Chemical structure of regioregular poly(3-hexylthiophene-2,5-diyl), P3HT

PCBM

For the pure PCBM measurement a 0.1 w% PCBM solution in chlorobenzene was prepared and stirred over night. The material was handled inside the glovebox. Afterwards the solution was diluted 1: 33 and sealed for the measurement.

For the ZnPc quenching measurement a 0.1 w% solution in toluene was prepared.

For the quenching measurement of MDMO – PPV a 0.1 w% solution of PCBM in chlorobenzene was prepared and for the quenching measurement of P3HT a 0.1 w% solution of PCBM in CHCl$_3$ was prepared.

The chemical structure of PCBM can be seen in Figure 2. 15.
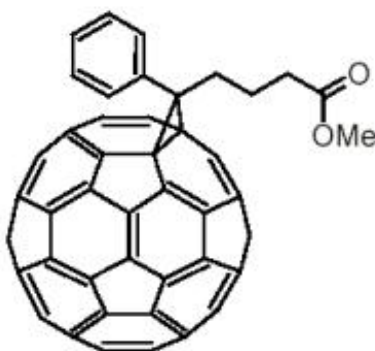
Figure 2. 15 Chemical structure of 1-(3-methoxycarbonyl) propyl-1-phenyl [6,6]C$_{61}$; PCBM

ZnPc

The Zincphthalocyanine solution was 0.01 w% in toluene and was diluted 1: 4 for the measurement. For a further measurement ZnPc was dissolved in chloroform (~ 0.1 w%).
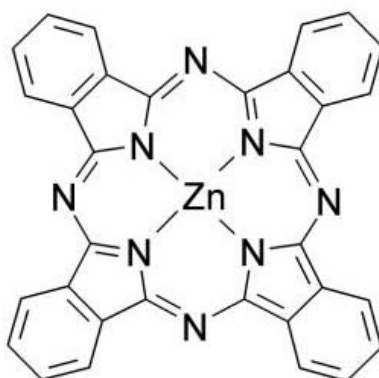
Figure 2. 16 Chemical structure of Zincphthalocyanine; ZnPc

TP 599

Two different solutions of this material were investigated. The first solution contained 1 mg TP599 in 1 ml toluene and the second one contained the same amount of TP599 in dichloromethane. The chemical structure of TP599 can be seen in Figure 2.17. The material was produced by P. Troshin from the RAS in Chernogolovka.[10]
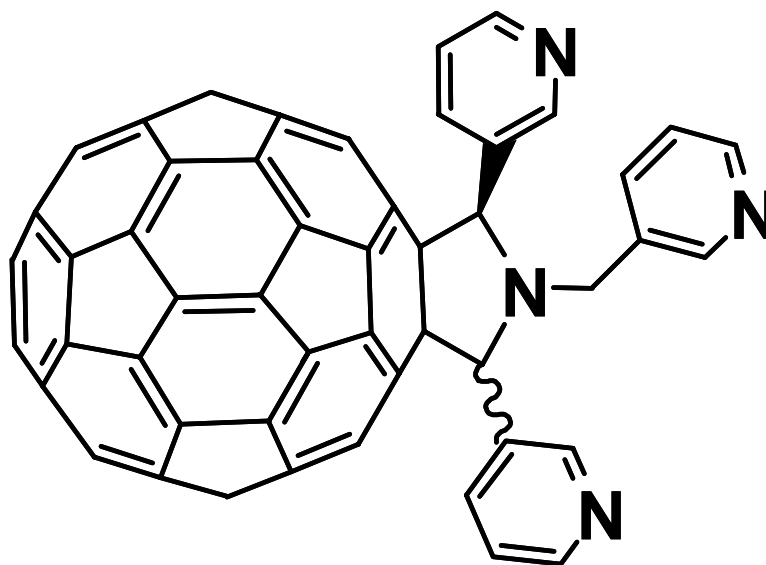
Figure 2. 17 Chemical structure of TP 599

Chapter 3

3 Results and Discussion

3.1. Measurements of system parts of the LP920

3.1.1. Effect of the manual irises

This experiment was performed to see the effect of closing or opening the manual irises 2.1.1.8 on the signal. For this purpose the Xe lamp was run in the CW mode, the lamp shutter was timed automatically in the 1Hz mode. The lamp was operated with 30 W and the measurement was done at 1480 nm and with a bandwidth of 0.7. An OD 1 filter was put inside the sample chamber after iris 2 (Figure 3. 1).

Figure 3. 1 Top view of the sample compartment

The results can be seen in the following table. ¼ means that the iris is closed to about ¼ , the same is true for the other values given in the table. The detector signal was taken at 10 ms.

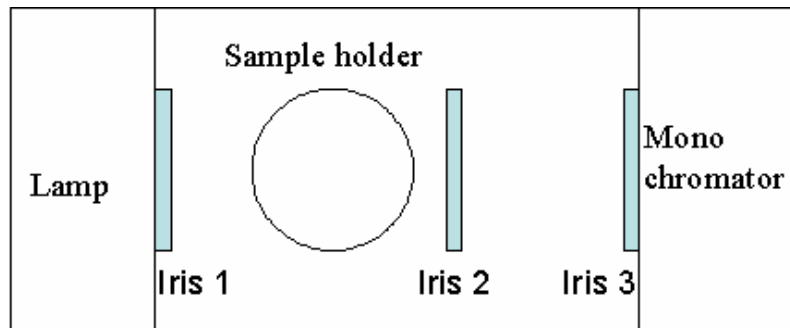| Iris 1	Iris 3	Iris 2	Detector signal [Volts[
open	open	open	7.1×10^{-3}
1/4	open	open	7×10^{-3}
1/2	open	open	6.9×10^{-3}
3/4	open	open	4.7×10^{-3}
1	open	open	0
open	1/4	open	6.8×10^{-3}
open	1/2	open	6.78×10^{-3}
open	3/4	open	6.76×10^{-3}
open	1	open	6.8×10^{-4}
open	open	1/4	7.1×10^{-3}
open	open	1/2	6.96×10^{-3}
open	open	3/4	4.03×10^{-3}
open	open	1	4.2×10^{-4}
3/4	3/4	3/4	3.06×10^{-3}
3/4	3/4	1/2	3.24×10^{-3}
3/4	3/4	open	3.30×10^{-3}
3/4	1/2	3/4	3.48×10^{-3}
3/4	1/4	3/4	3.24×10^{-3}
3/4	open	3/4	3.44×10^{-3}
1/2	3/4	3/4	4.12×10^{-3}
1/4	3/4	3/4	4.18×10^{-3}
open	3/4	3/4	3.94×10^{-3}
1/2	open	1/2	6.9×10^{-3}
1/2	open	1/4	7.22×10^{-3}
1/2	open	3/4	4.32×10^{-3}
1/4	open	1/2	7.32×10^{-3}
3/4	open	1/2	4.4×10^{-3}

It can be seen quite clearly that has closing the iris 1 and 3 leads to the largest changes. Iris 2 has only a very small effect on the signal.

It was found out that for PL measurement it is the best way to close iris 2 to about ¾ to get rid of the scattered laser light. For Absorption measurements the iris 2 should be opened fully.

Iris 1 and 3 were in all cases adjusted so that way, that the signal to noise ratio was optimal. In nearly all cases it was best to close these two irises to about ¾.

3.1.2. Saturation curves of the detectors

This experiment was performed to see the saturation curve for the NIR detector, because nothing was known about this detector. The PMT has a detection limit of 1.2 V and that signals with higher values won't be detected. There are no problems with saturation in the PL measurement because the signals are rather small. This means, the problems of saturating the detector mostly occur in absorption measurements, because the background level of the Xe lamp is quite high. For that purpose, adjusting the irises is very important. One has to look in the setup mode over the whole spectrum range, that no signal is going up to the saturation limit of the detector.

The experiment was performed at 30 W lamp power and at 108 W lamp power. The pulse width was 10 ms and the detection wavelength 1480 nm. The lamp was operated in the CW mode and the shutter was timed. The bandwidth at the experiment was 2.For reducing the lamp power filters were used (OD 1, OD 0.6, OD 2, OD 3). The time range was 20 ms and the voltage range was set to 160 mV. It might be that the filters are not be specified for that wavelength.

Power	Detector signal [V]
30 W OD3	5.2×10^{-4}
30 W OD2	6.0×10^{-3}
30 W OD1	3.3×10^{-2}
30 W OD 0.6	4.6×10^{-2}
30 W	9.6×10^{-2}
42 W	9.6×10^{-2}
54 W	9.6×10^{-2}
108 W	9.6×10^{-2}

It was found out that the saturation value for the NIR detector is around 9.6×10^{-2} V.

3.2. Investigated Materials

3.2.1. C_{60}

The transient absorption of a C_{60} solution in toluene was measured. To detect the lifetime of the triplet state a multiple measurement at 400 nm has been done. The system was run at 10 Hz doing 16 averages with the oscilloscope. For the measurement two traces were collected, both with a background correction. The time range was 40 μs and the voltage range 40 mV. The bandwidth was set to 0.5. The excitation wavelength was 355 nm.

The lifetime was 6275 ns, which fist quite well to the data in the literature. The values given in some papers are measured in Ar saturated and in air saturated solutions. The lifetime which was achieved with this measurement is 1 order of magnitude lower than for an Ar saturated solution and one order of magnitude higher than for a air saturated solution. The effect of air is due to a effective quenching of the triplet state by $^{3}O_{2}$. [8] Therefore it can be assumed that some air diffused into the solution. (Figure 3. 2)
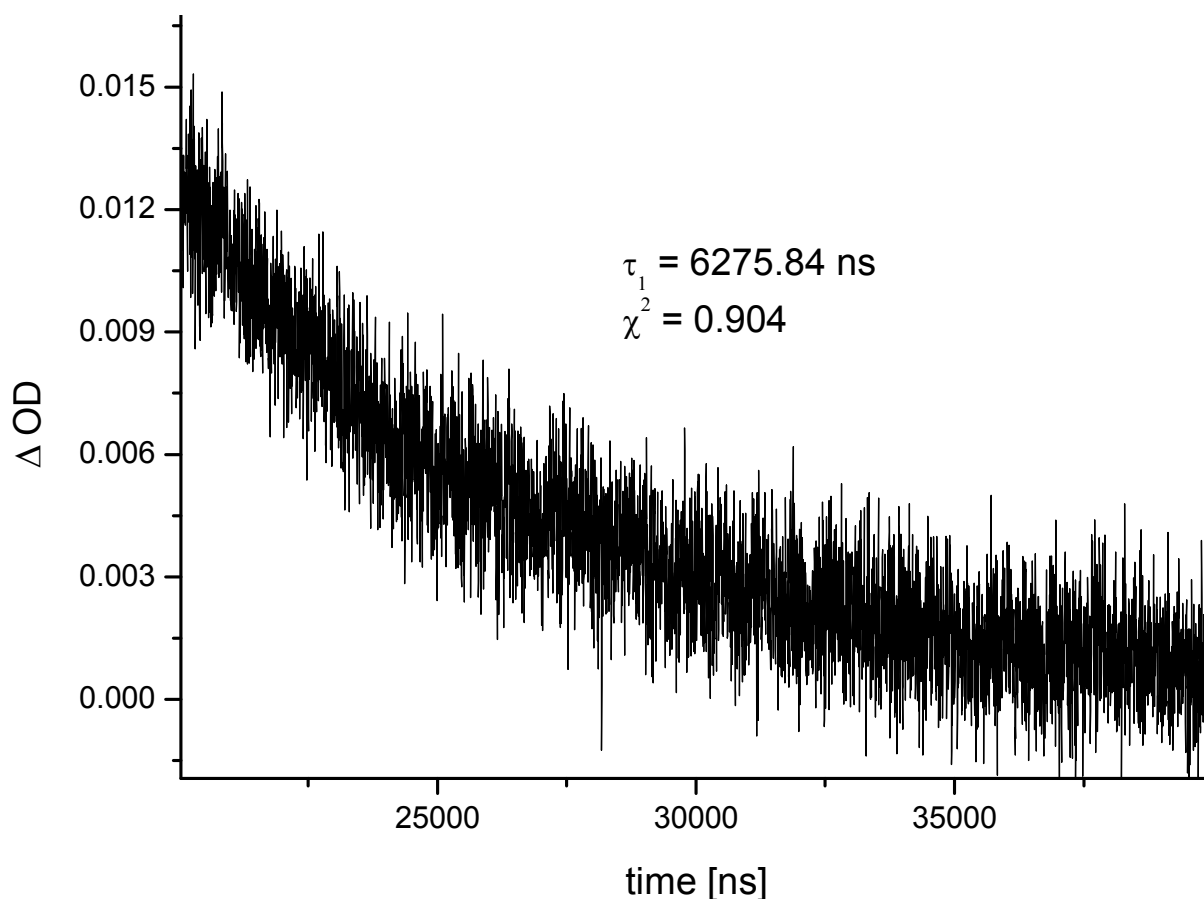
τ_1 = 6275.84 ns

χ^2 = 0.904

Figure 3. 2 Triplet absorption decay of C_{60} at 400 nm

Two map measurements of the C_{60} solution were also carried out.

The first one covered a wavelength range from 400 to 670 nm. The spectrum was measured in 5 nm steps. The map was measured in the 10 Hz mode with 16 averages, each single trace was measured 3 times, and then the average of these 3 shots was taken as one single trace. The time range was 40 μs and the voltage range 40 mV. The bandwidth was set to 0.5. The traces of the map can be seen in Figure 3.3 b, some special traces were choose to be plotted in Figure 3.3a for a better comparison. The different traces represent different wavelength. According to the lamp profile the background level of the lamp is different for different wavelength. Therefore each trace has a different onset. By calculating the Δ OD one can get rid of this effect. The calculated Δ OD in Figure 3.4(only for some traces) and the sliced spectrum at 20 μs in Figure 3. 5. This spectrum is according to literature [8,9] the $T_1 - T_N$ transition of C_{60}. The transitions of the T_N states are so close to each other that the different states can not be resolved.
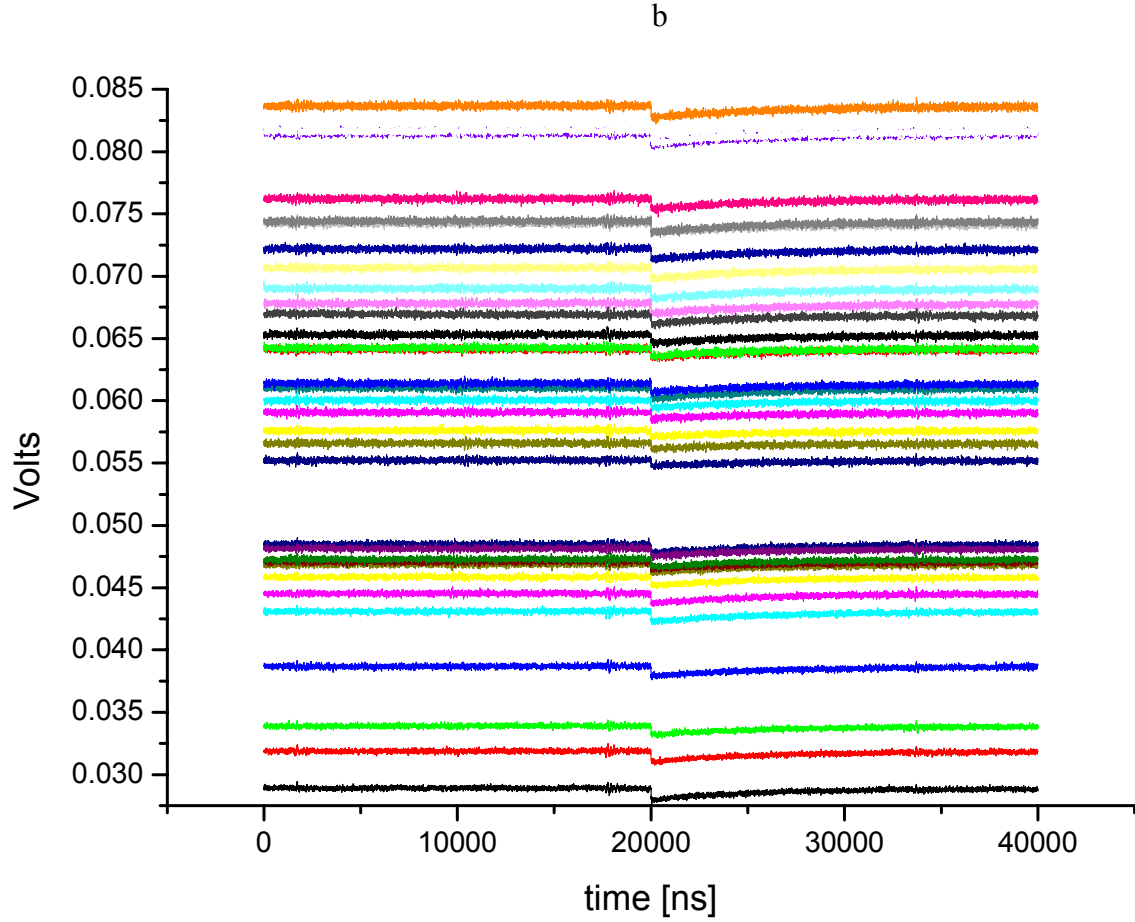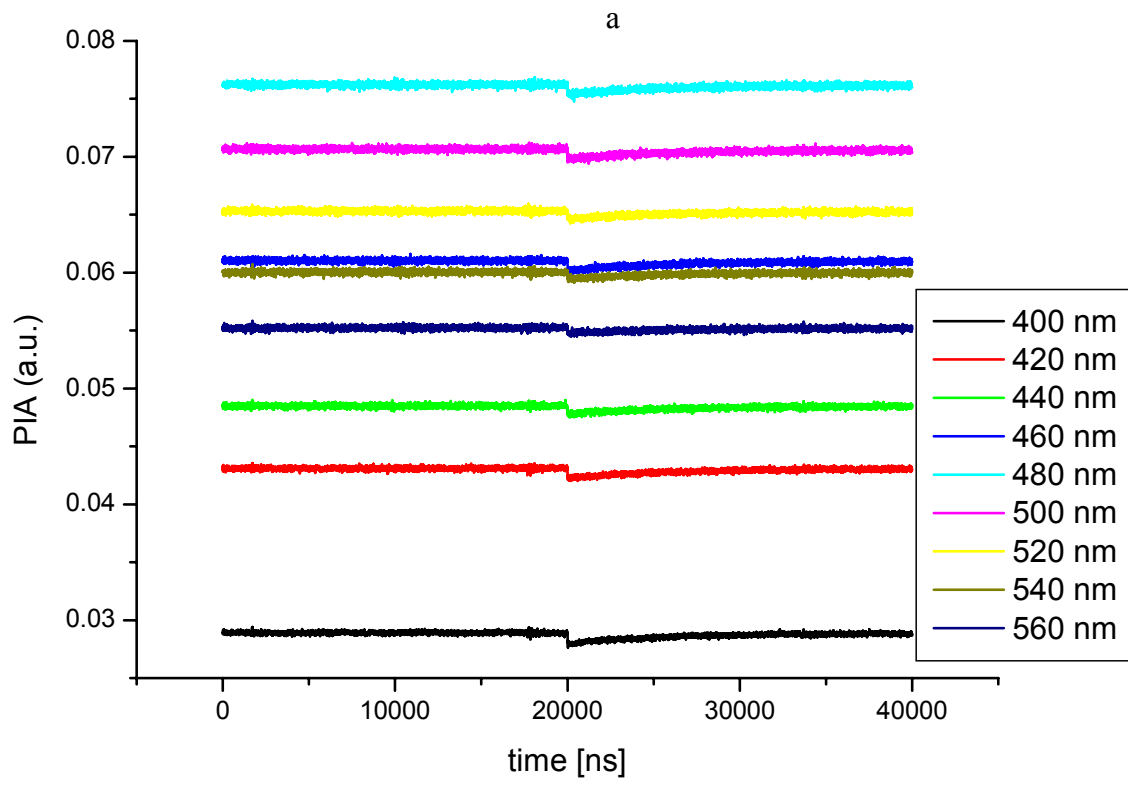
Figure 3. 3 (a) Some traces of the $T_1 - T_N$ absorption of C_{60} in solution

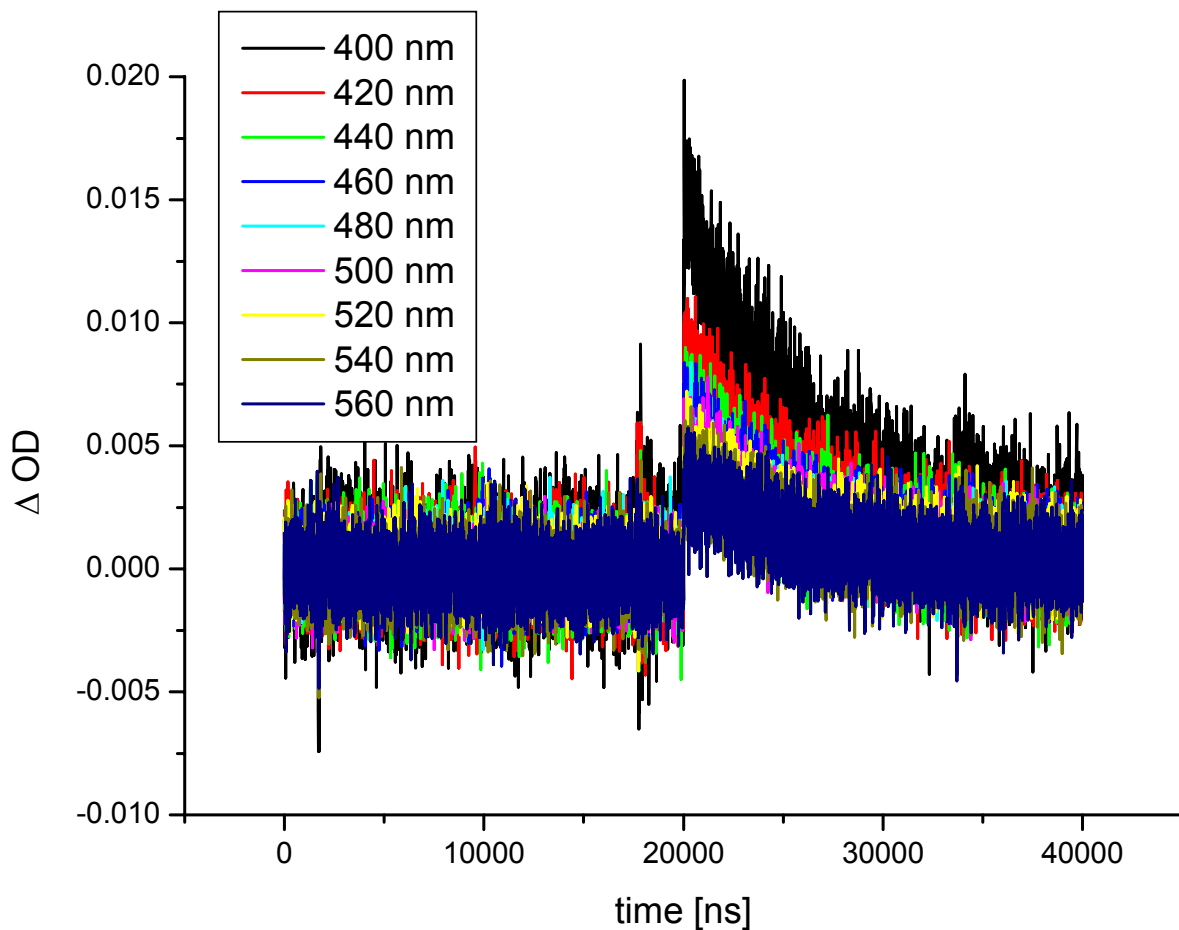(b) All traces of the $T_1 - T_N$ absorption of C_{60} in solution

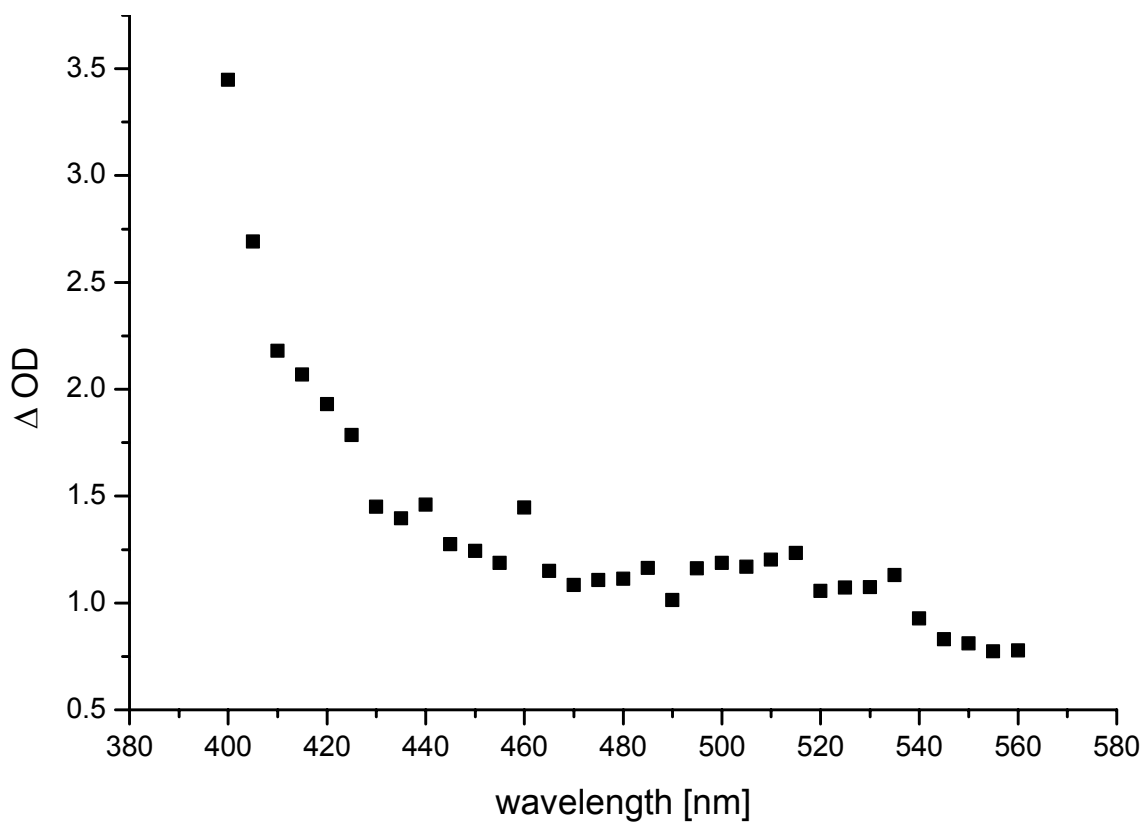Figure 3. 4 The Δ OD traces of the $T_1 - T_N$ absorption of C_{60} in solution

Figure 3. 5 The $T_1 - T_N$ absorption spectrum of C_{60} in solution sliced at 20 µs

The second absorption spectrum which was measured covered a wavelength range from 640 to 790 nm. The spectrum was taken with 6 nm steps. Once again the spectrum was measured in the 10 Hz mode, doing 16 averages and 3 shots per step. The voltage range was set to 40 mV and the time range to 40 μs. The bandwidth was 0.5.

Some of the absorption traces can be seen in Figure 3.6 and the Δ OD traces in Figure 3.7. The resulting spectrum (sliced at 20 μs) can be seen in Figure 3.9. Again the different colours represent different wavelength.

The maximum lays around 750 nm. According to the values in the literature the spectrum can be associated to the $T_1 - T_2$ transition of C_{60} (1.68 eV). [9]

The lifetime of the excited state was calculated by extracting the trace at 750 nm. The lifetime is 5100 ns. (Figure 3. 9)
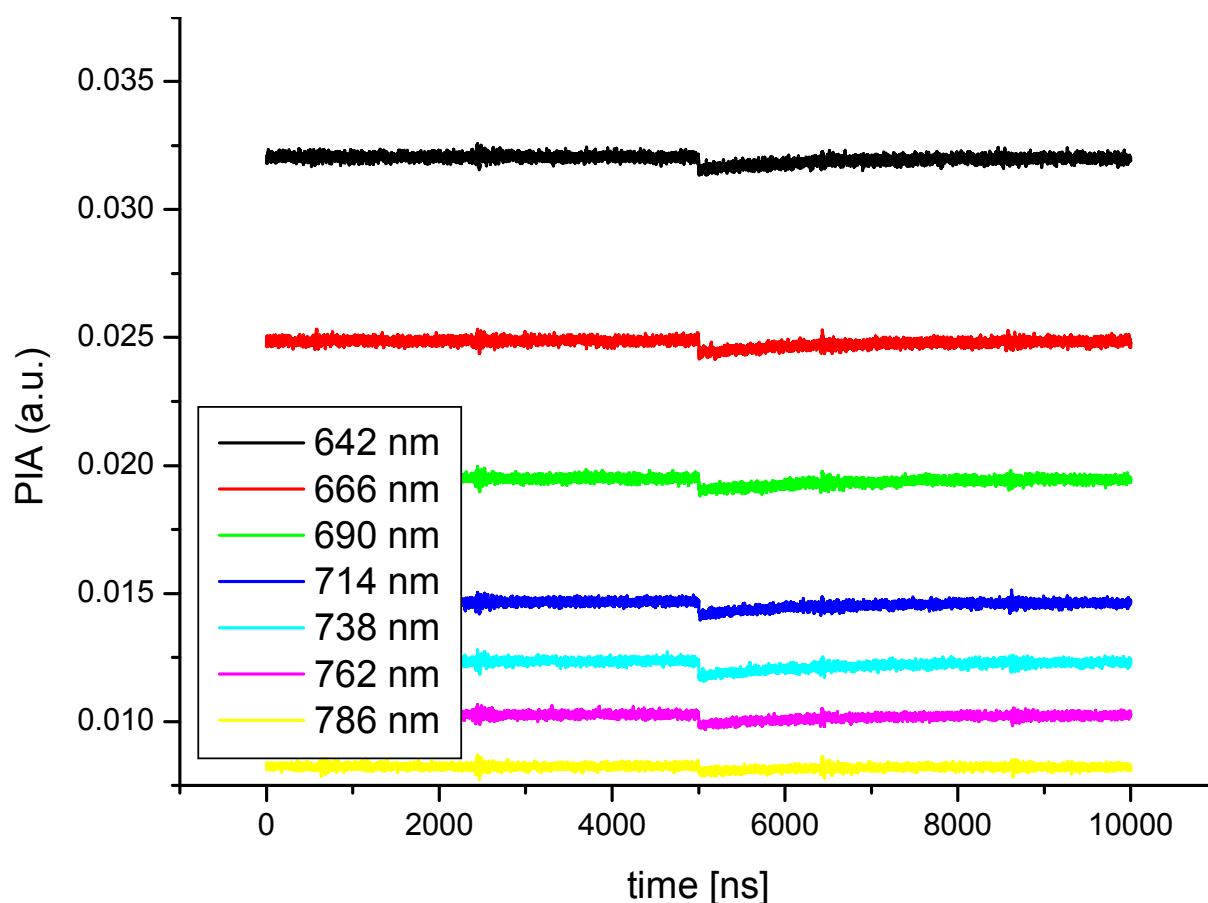

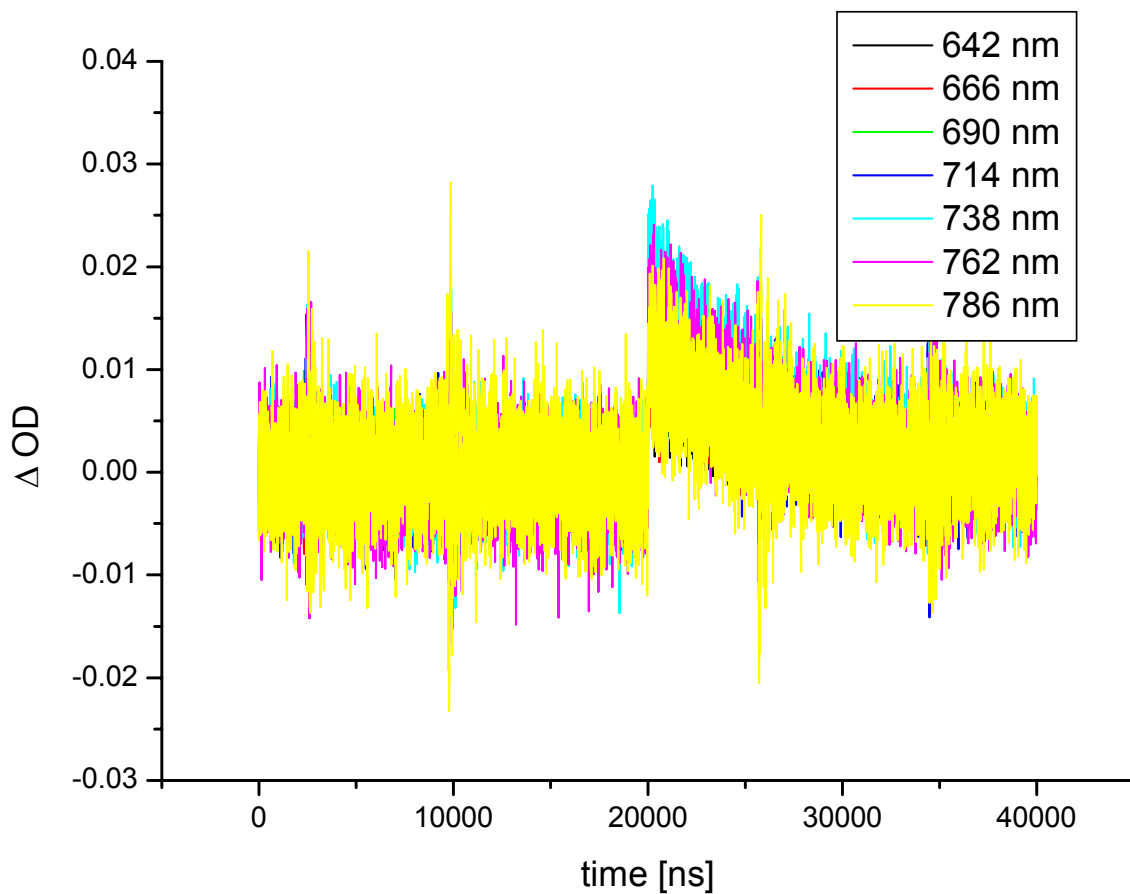Figure 3. 6 Absorption traces of the $T_1 - T_2$ transition of C_{60} in solution

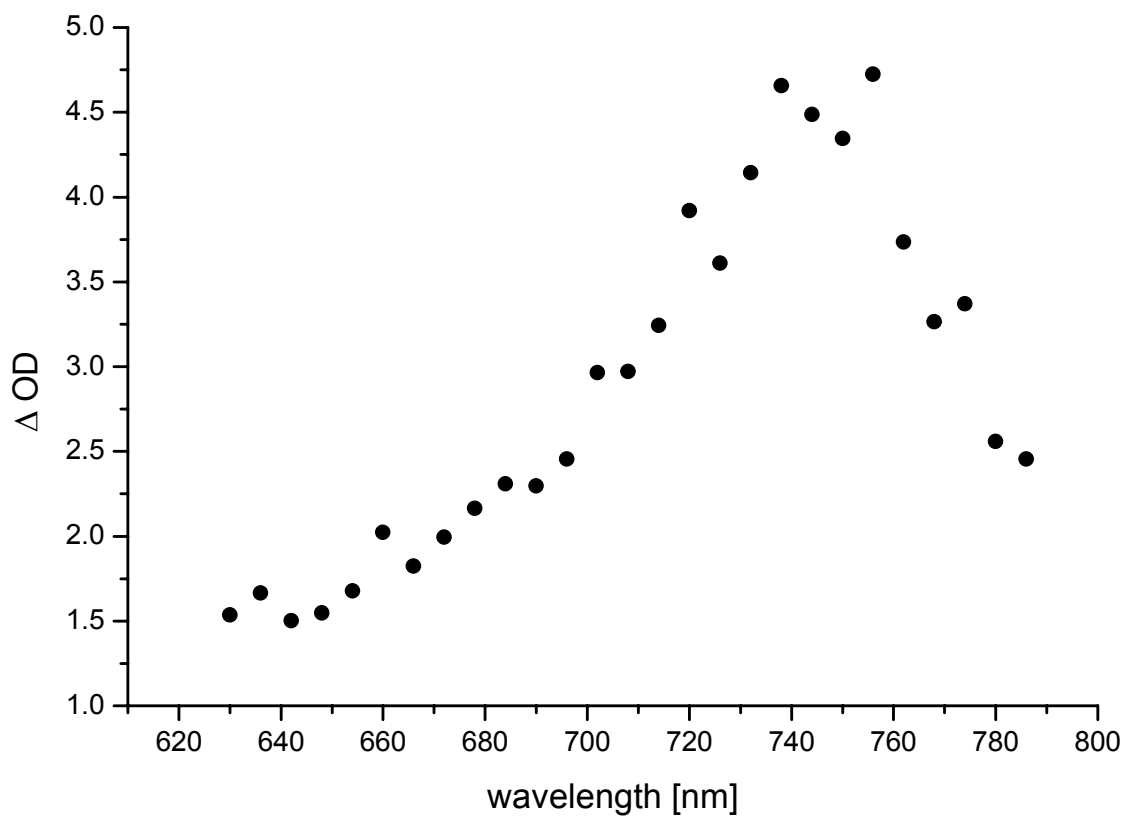Figure 3. 7 The Δ OD traces of the $T_1 - T_2$ transition of C_{60} in solution

Figure 3. 8 Sliced spectrum of the $T_1 - T_2$ transition of C_{60} in solution sliced at 20 µs
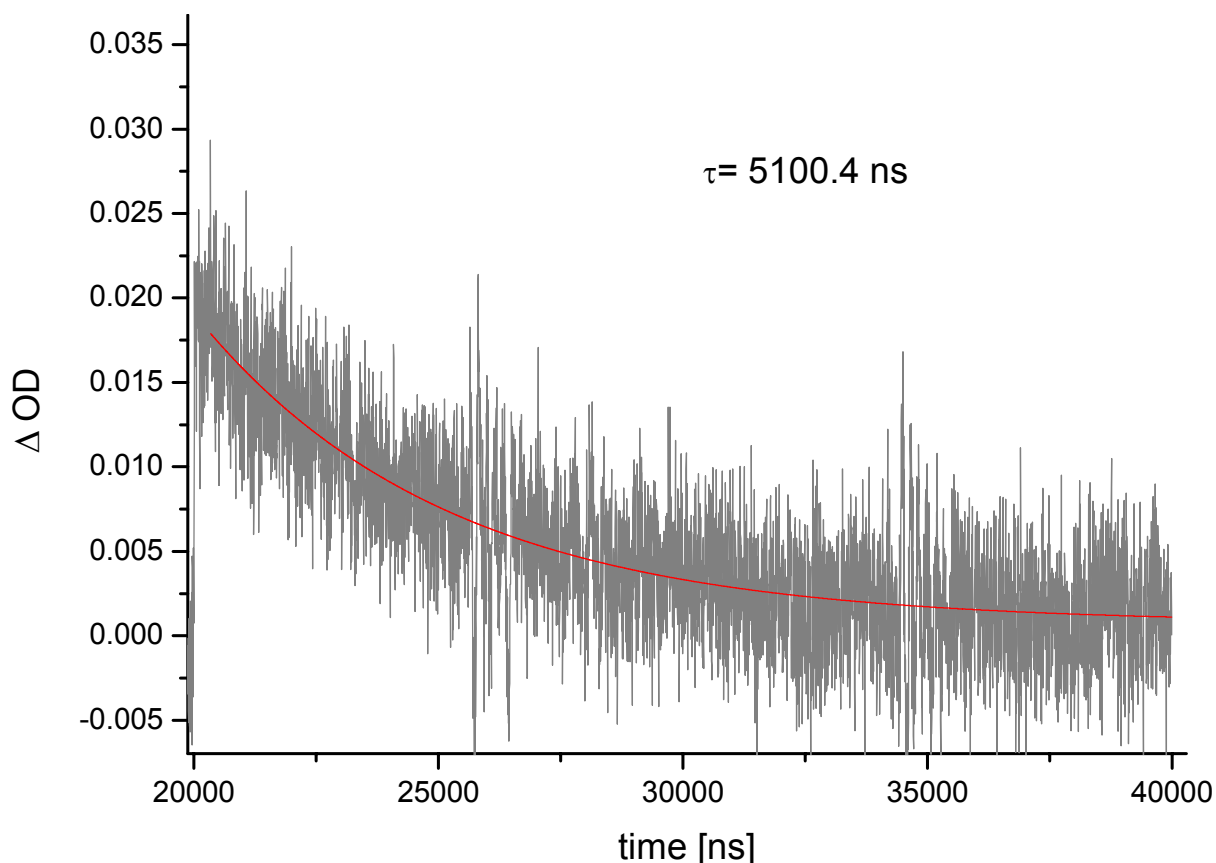
τ= 5100.4 ns

Figure 3. 9 Trace at 750 nm for the calculation of the lifetime

3.2.2. PCBM

Two absorption map measurements of a PCBM solution were carried out. In both cases the excitation wavelength was 355 nm.

The first one covered a wavelength range from 350 to 580 nm. The time range was set to 4 ms and the voltage range to 80 mV. The map was measured in the 10 Hz mode doing 32 averages. Each trace was measured 4 times and then averaged. The bandwidth was set to 1.5. In this section only the spectra and the lifetime fits are shown. (Figure 3. 10)

At 375 nm, the trace was extracted and afterwards the lifetime was calculated. The lifetime is 348 ns. (Figure 3. 11)

PCBM is from the structure very close to the C_{60}, only an additional side chain is present, to provide the better solubility of PCBM compared to C_{60} it can be assumed that this spectrum is comparable to the C_{60} spectrum at the same wavelength range.

The difference in the lifetime might come from diffused air into the solution, because the lifetime of 348 ns is quite close to the literature data for an air saturated C_{60} solution. [9]
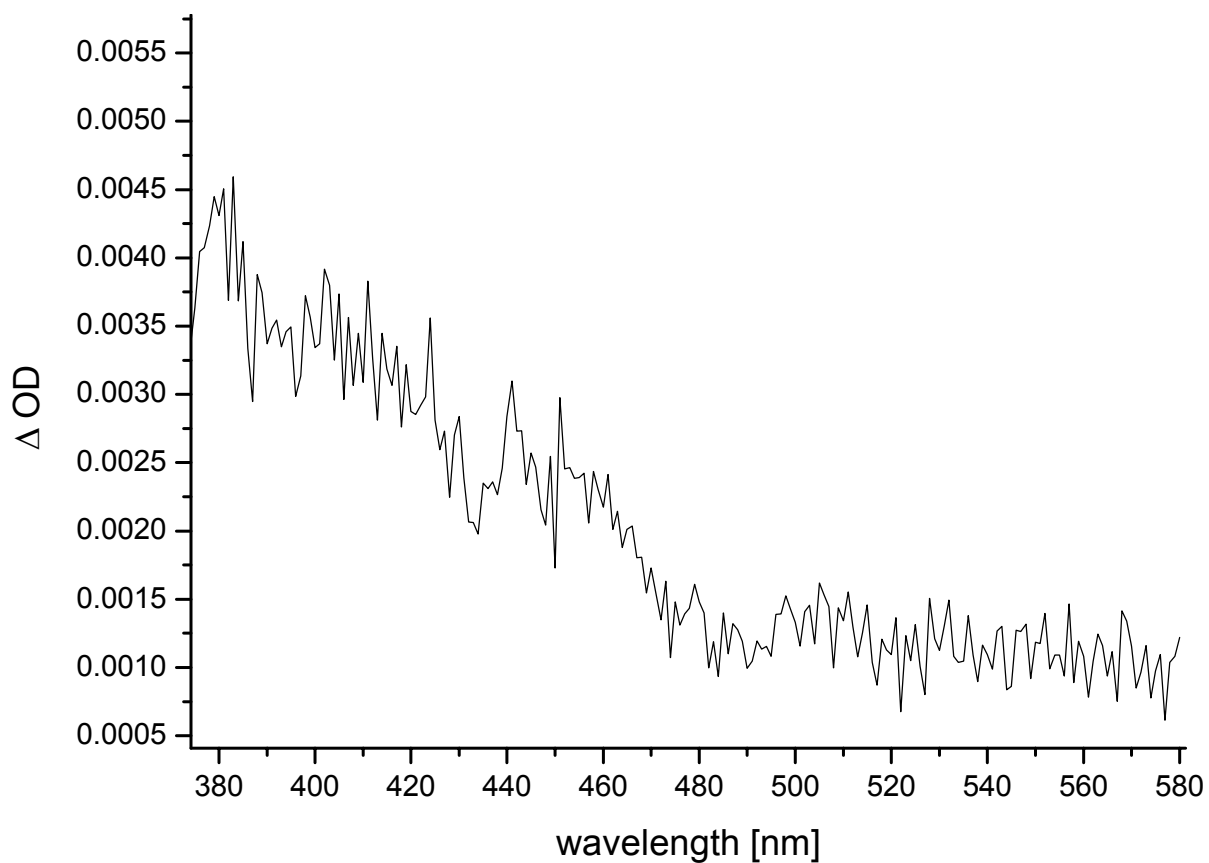
Figure 3. 10 Spectrum of PCBM in solution from 350 to 750 nm sliced at 20 µs
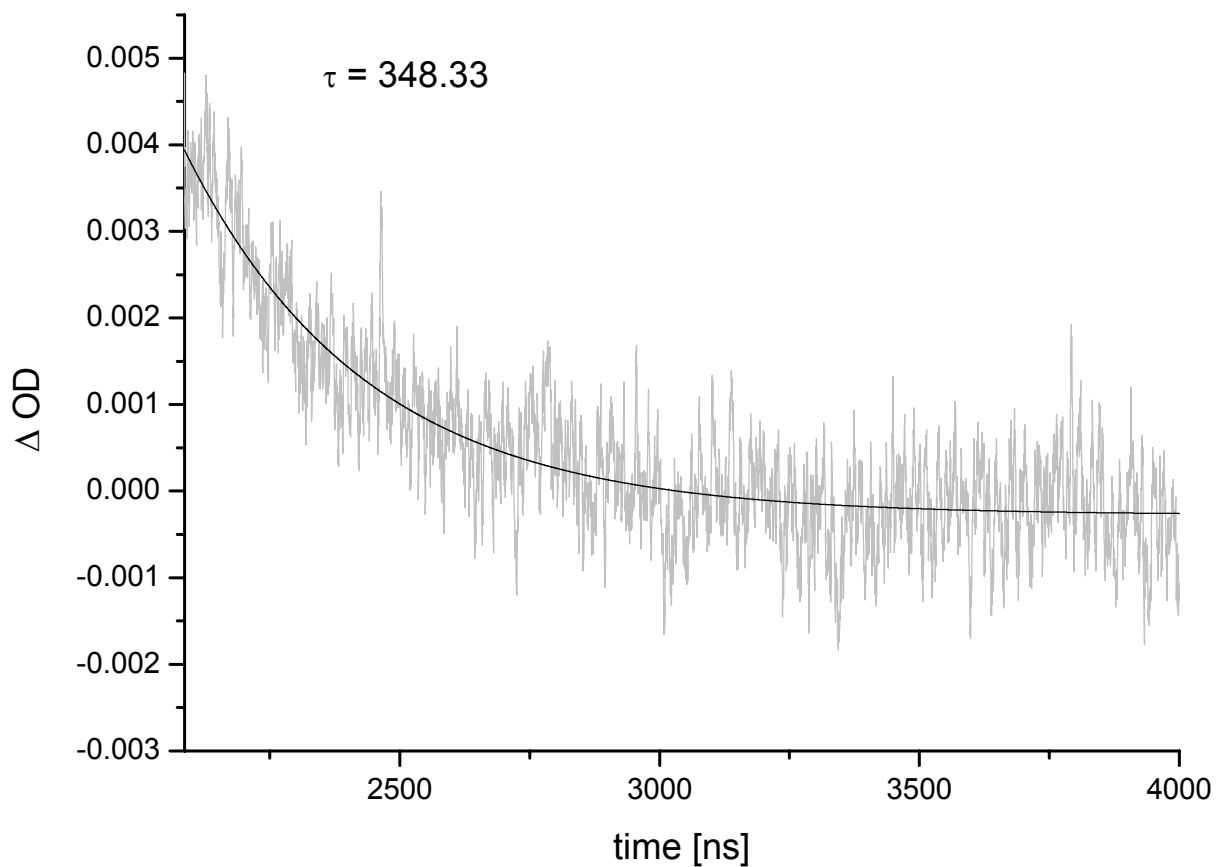
Figure 3. 11 Extracted trace at 375 nm and lifetime calculation

46

The second map measurement of the PCBM solution covered a wavelength range from 530 to 800 nm. The spectrum was measured with a time range of 4000 ns and a voltage range of 80 mV. The map was taken with 3 shots per step with 1 nm steps. The repetition rate was 10 Hz doing 32 averages. The bandwidth was set to 1.5.

For the lifetime calculation the trace at 700 nm was extracted. The lifetime is 352 ns. Due to the structural similarity of PCBM and C_{60} it can be assumed that the measured spectrum is the $T_1 - T_2$ transition. The much shorter lifetime is again correlated with the diffusion of air into the solution.

Figure 3. 12 Spectra of the T_1 - T_2 transition of PCBM in solution sliced at 20 μs
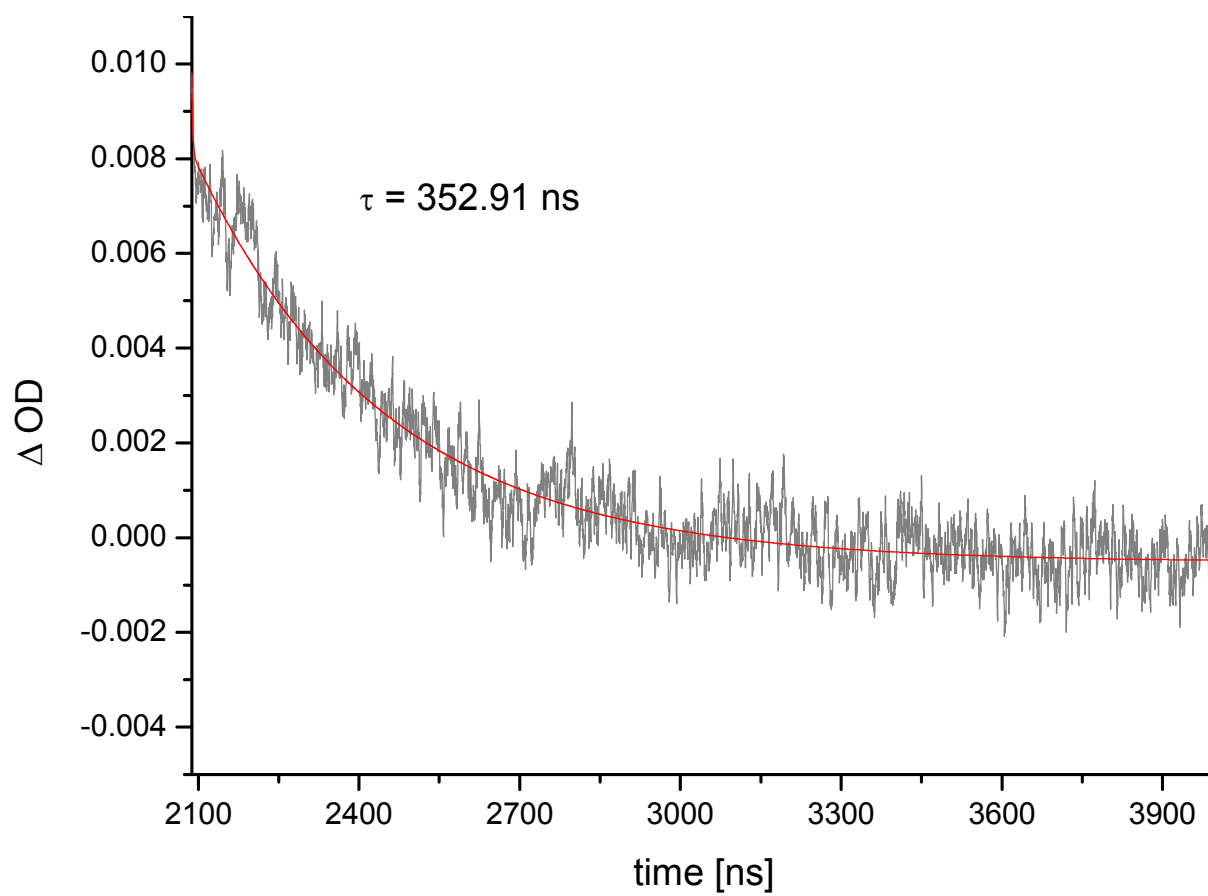
Figure 3. 13 Trace at 700 nm for the calculation of the lifetime

3.2.3. MDMO – PPV

A lot of time resolved luminescence studies on PPV and related compounds [13,14,15,16,21] and transient PIA studies in combination with PCBM [17,18,19,20] have already been carried out.

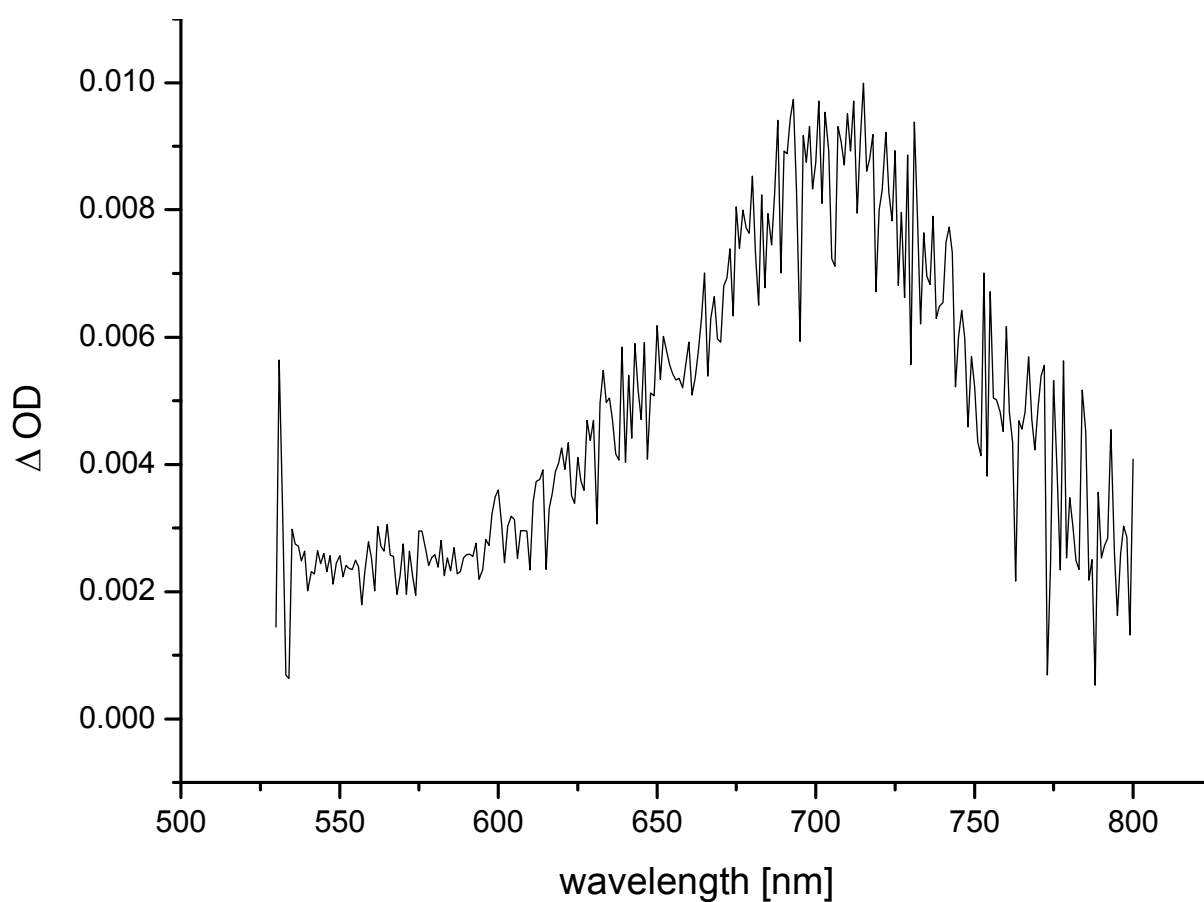The photoluminescence spectrum of MDMO – PPV was taken in the wavelength range from 510 to 740 nm. The bandwidth was 1. The voltage range was 1600 mV and the time range 200 ns. The map was measured in the 10 Hz mode doing 32 averages and 5 shots per step. (Figure 3. 14)

The lifetime couldn't be calculated because it is too close to the detection limit of the system which is around 5 ns. The excitation wavelength was 532 nm.

For this measurement no filter was used because after adjusting the iris at the sample holder there was no more influence of scatter laser light.

The maximum of the peak is at 563 nm and the spectrum shows one shoulder between 580 to 620 nm. The peak maximum is red shifted compared to literature data for films where the maximum is below 600 nm [11].
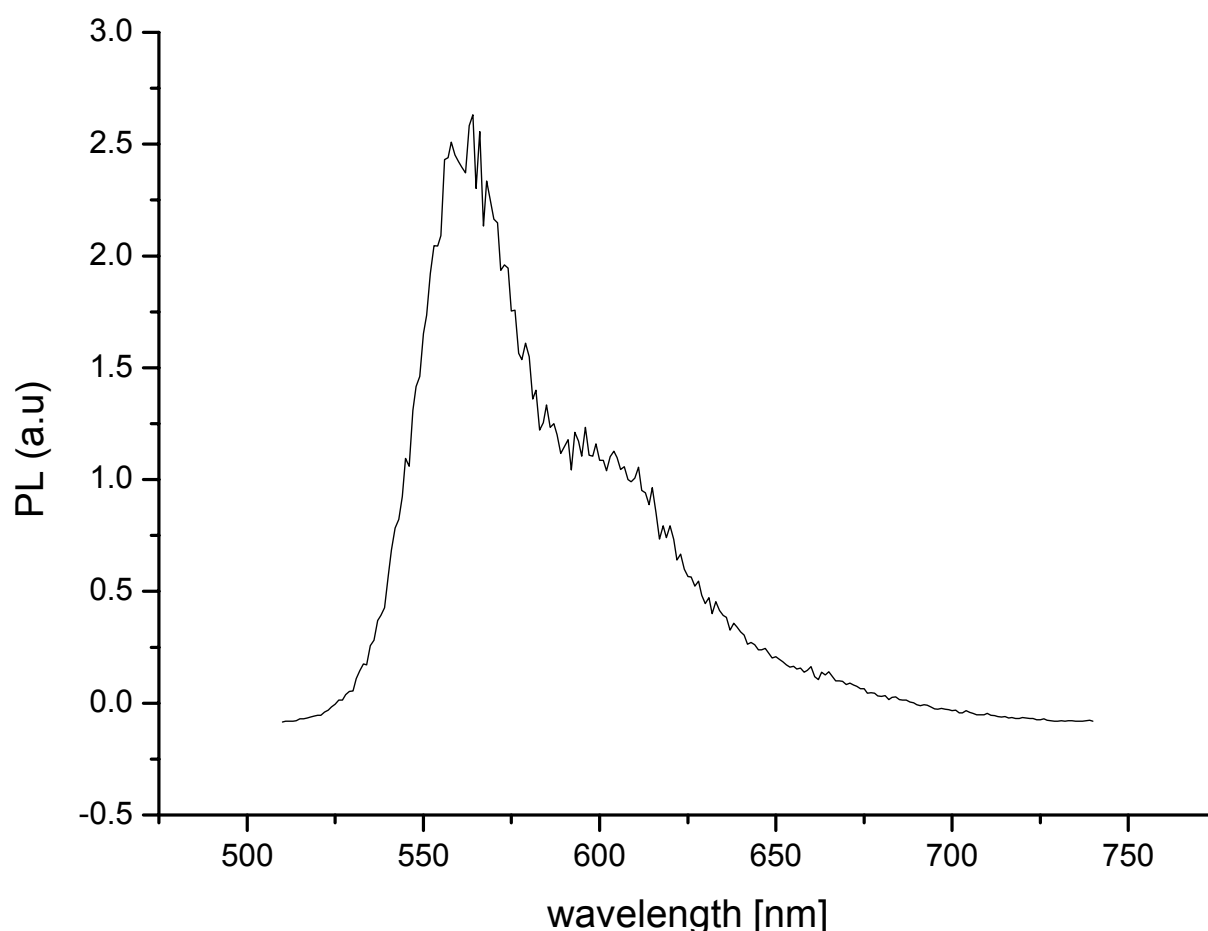
Figure 3. 14 Transient PL spectrum of MDMO – PPV in solution

The second part of the MDMO – PPV measurements was a quenching measurement. The quencher was a 0.1 w% solution of PCBM in chlorobenzene. The measurements were carried out in the wavelength range between 510 and 750 nm. The filter for the 532 nm was used. The maps were measured in the 10 Hz doing 32 averages. The spectra were taken in 2.5 nm steps, each trace measured 5 times and then averaged. The bandwidth was set to 0.8. The voltage range was 800 mV and the time range 400 ns.

First a spectrum of the pure MDMO – PPV solution was measured. Then the 0.1 w% PCBM solution was added in 20 µl steps which corresponds to the addition of 20 µg (1.1 x 10^{-5} mol/l). All together 280 µl of PCBM solution were added, this is equivalent to 1.33 x 10^{-4} mol/l PCBM solution. (Figure 3. 15)

Afterwards the values of the peak maximum at 562.5 nm were taken used to get a Stern – Volmer plot.(Figure 3. 16)
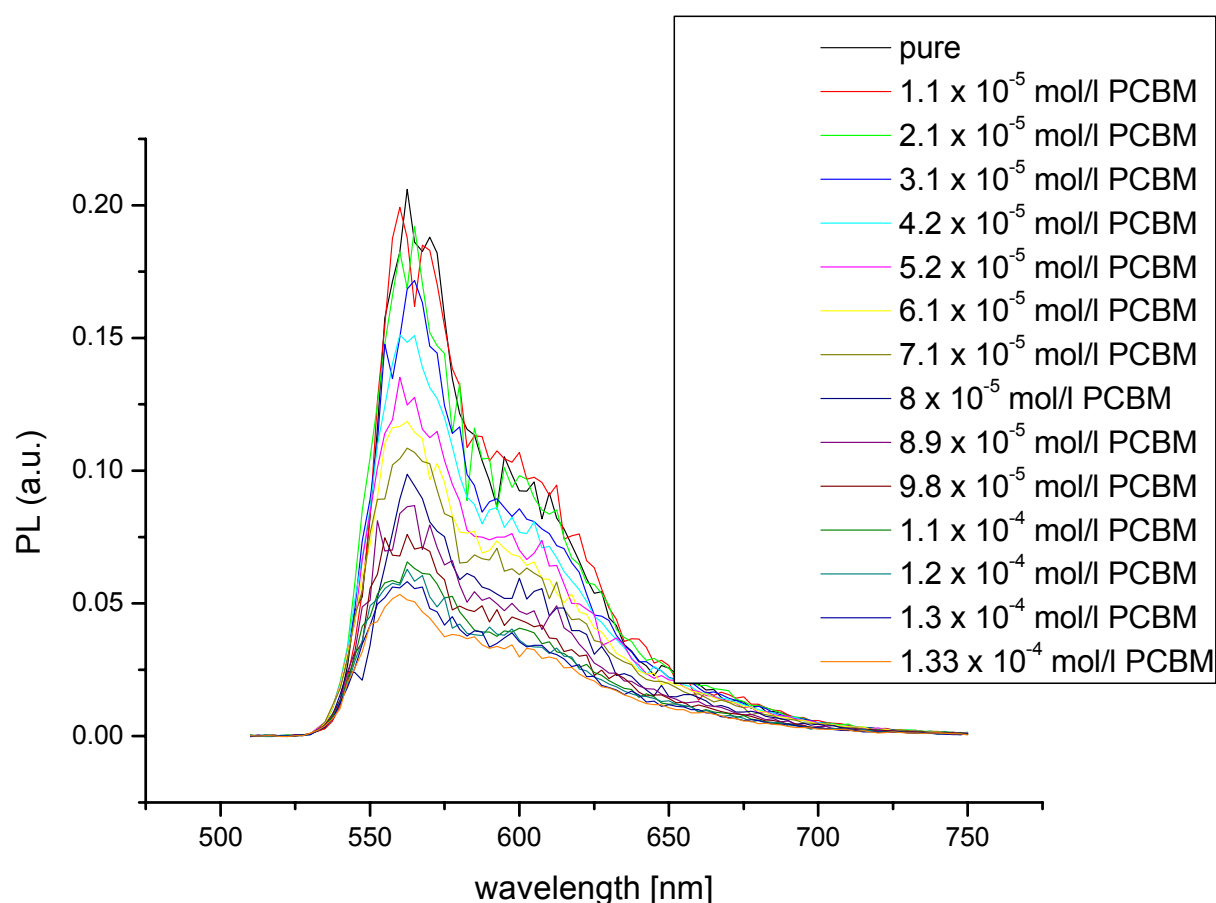
Figure 3. 15 Spectra of the MDMO – PPV solutions with PCBM
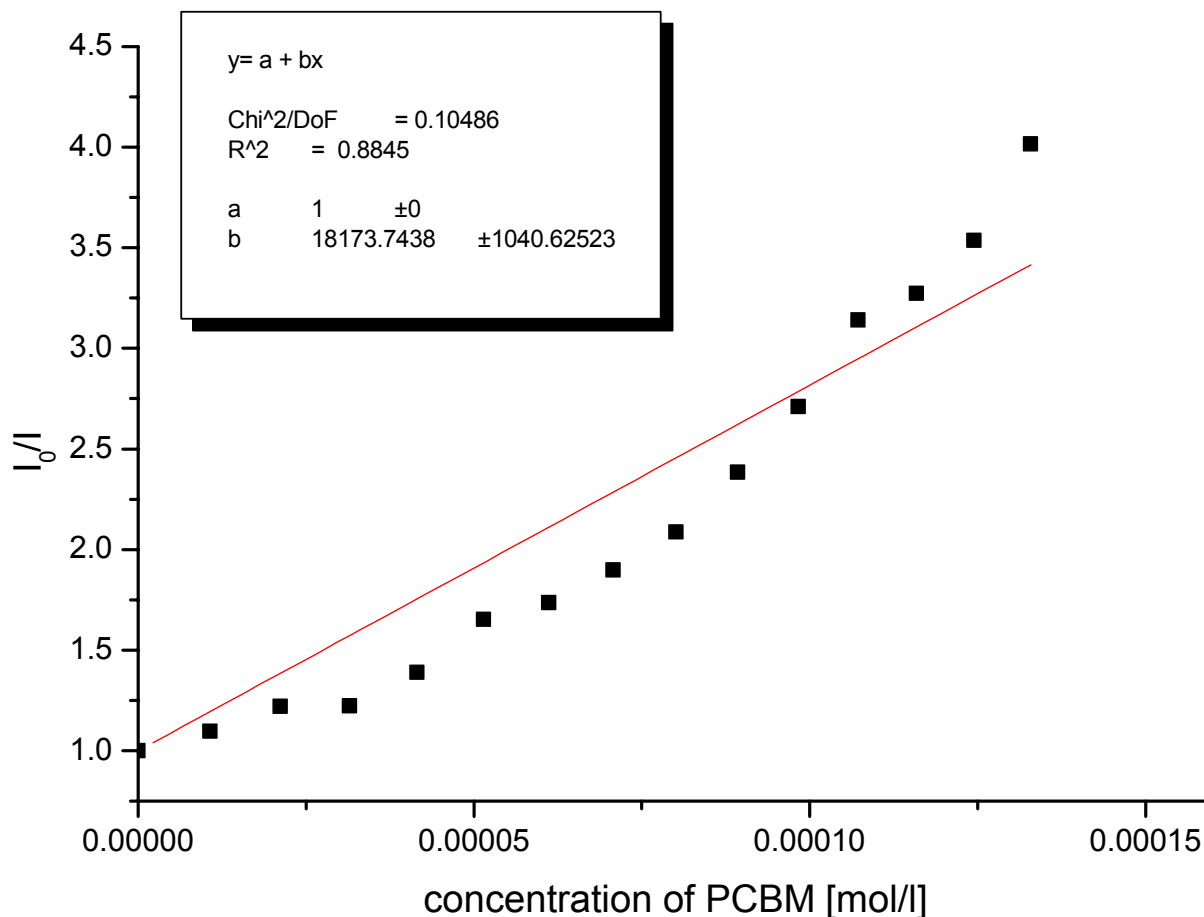
Figure 3. 16 Stern – Volmer Plot

It can be derived from Figure 3.17 that the PL is efficiently quenched by PCBM. As MDMO – PPV and PCBM is a well known system [22,23,24,27] and a lot of studies have been carried out it can be assumed that the quenching of the photoluminescence is due to an ultra fast electron transfer. [25,26,31]

As shown in equation 1.18 and 1.19 and in figure 1.6 the slope of the fit is the Stern – Volmer constant K_{SV}. K_{SV} in this experiment is $18x10^3$ l/mol, which is around one order of magnitude higher than the values in the literature for MEH-PPV [28]. Together with the $\tau_F \approx 300$ ps [12], the MDMO-PPV concentration of 0.02 mg/ml and $M_n \approx 300\ 000$ g/mol this leads to a value of $k_q \approx 4 \times 10^6$ s^{-1}. The given τ_F value is taken from MEH-PPV but according to their structural similarity it is assumed that the lifetimes of PL are more or less the same and the M_n value was given by the company [29].

The absolute values of the peaks were taken because it was not possible to monitor the decay by a reduced lifetime of the PL. This is due to the instrumental resolution of the system, which is around 5 ns. PL decays of conjugated polymers are usually much faster.

51

3.2.4. P3HT

Once again two kinds of measurements were carried out: the spectrum of the P3HT and a quenching measurement with PCBM.

The first measurement was the P3HT photoluminescence spectrum. This spectrum was taken in the wavelength range from 500 to 750 nm. The excitation wavelength was 532 nm and a corresponding filter was used. The time range was 200 ns and the voltage range 400 mV. The map was measured in the 10 Hz mode doing 32 averages. The spectrum was measured in 0.5 nm steps.

The maximum of the peak is at 579 nm. (Figure 3. 17) The derived spectrum is according to the literature. [30]
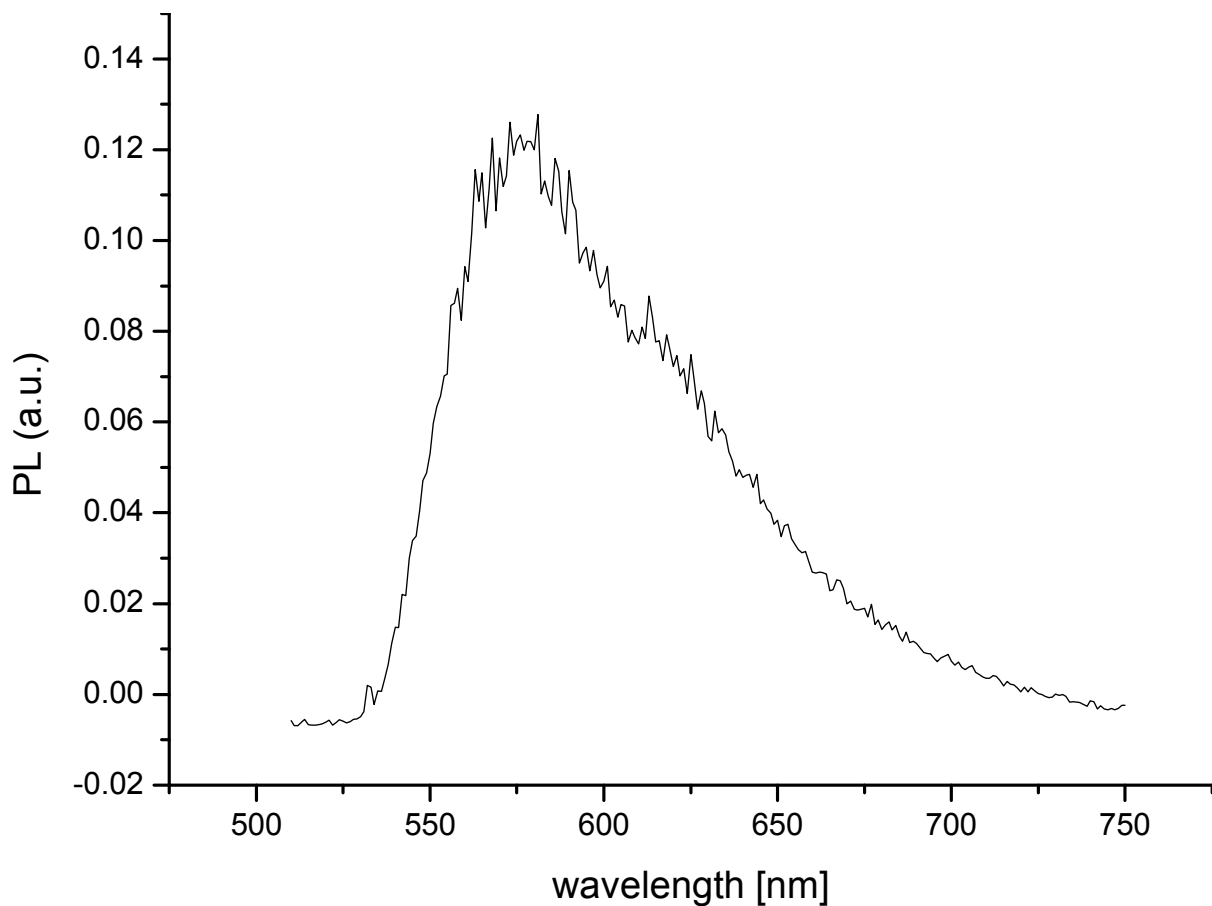
Figure 3. 17 Photoluminescence spectrum of P3HT in solution

The second part of the P3HT measurements was a quenching measurement. For that purpose a 0.1 w% PCBM solution in $CHCL_3$ was added in 20 µl (8.6 x 10^{-6} mol/l) steps to the pure P3HT solution. The excitation wavelength was 532 nm and the corresponding filter was used. The bandwidth was set to 0.8 and the wavelength range was from 710 to 740 nm. The map was taken in 2.5 nm steps and the system was run in the 10 Hz mode doing 32 averages. Each trace was measured 5 times and then averaged by the computer. The voltage range was set to 80 mV and the time range was 400 ns.

The total amount of PCBM added to the solution was 220 µl PCBM solution which corresponds to an 8.8 x 10^{-5} mol/l PCBM solution.

Afterwards the values of the spectra at 587 nm were taken and plotted in a Stern – Volmer plot.

Once again the absolute values were taken because the lifetime of the PL decay is below the time resolution limit of the system.
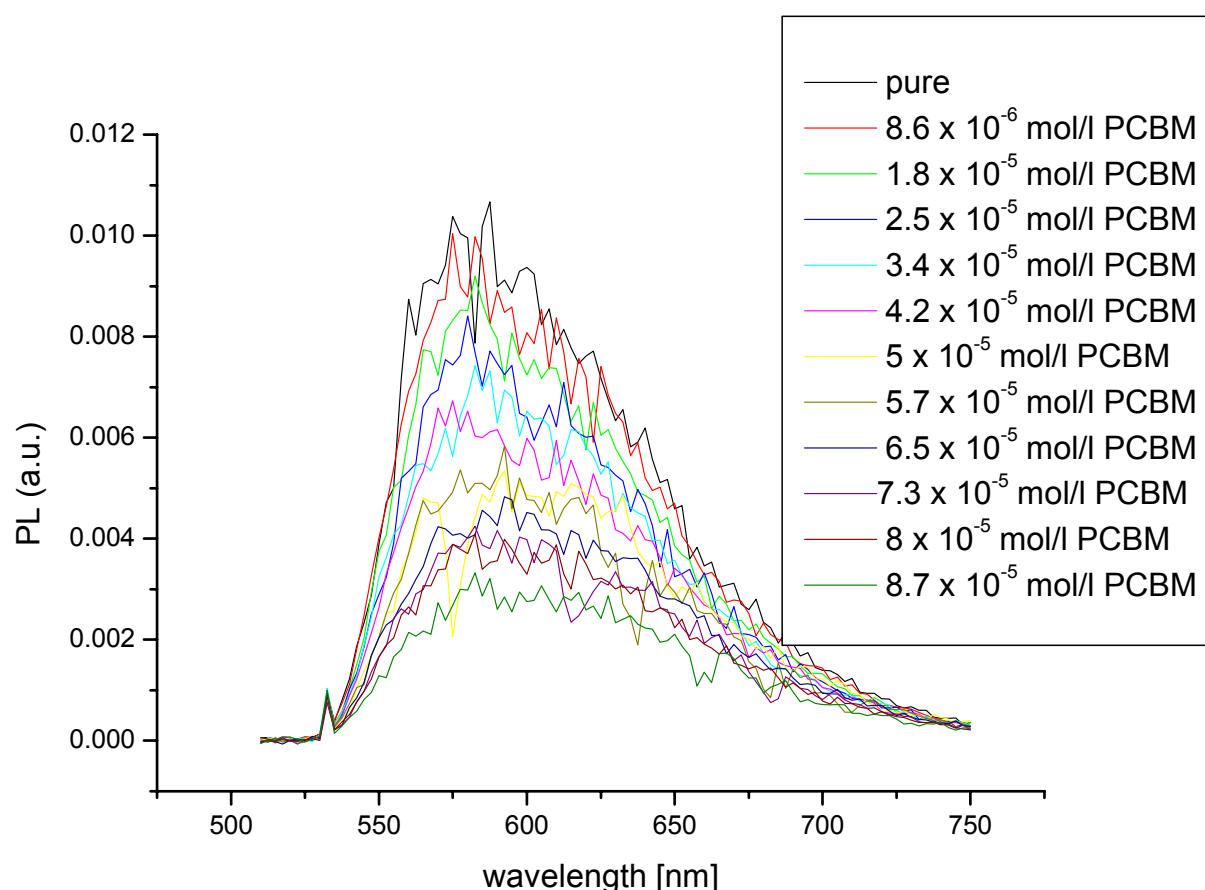
Figure 3. 18 Spectra of the P3HT solutions with PCBM
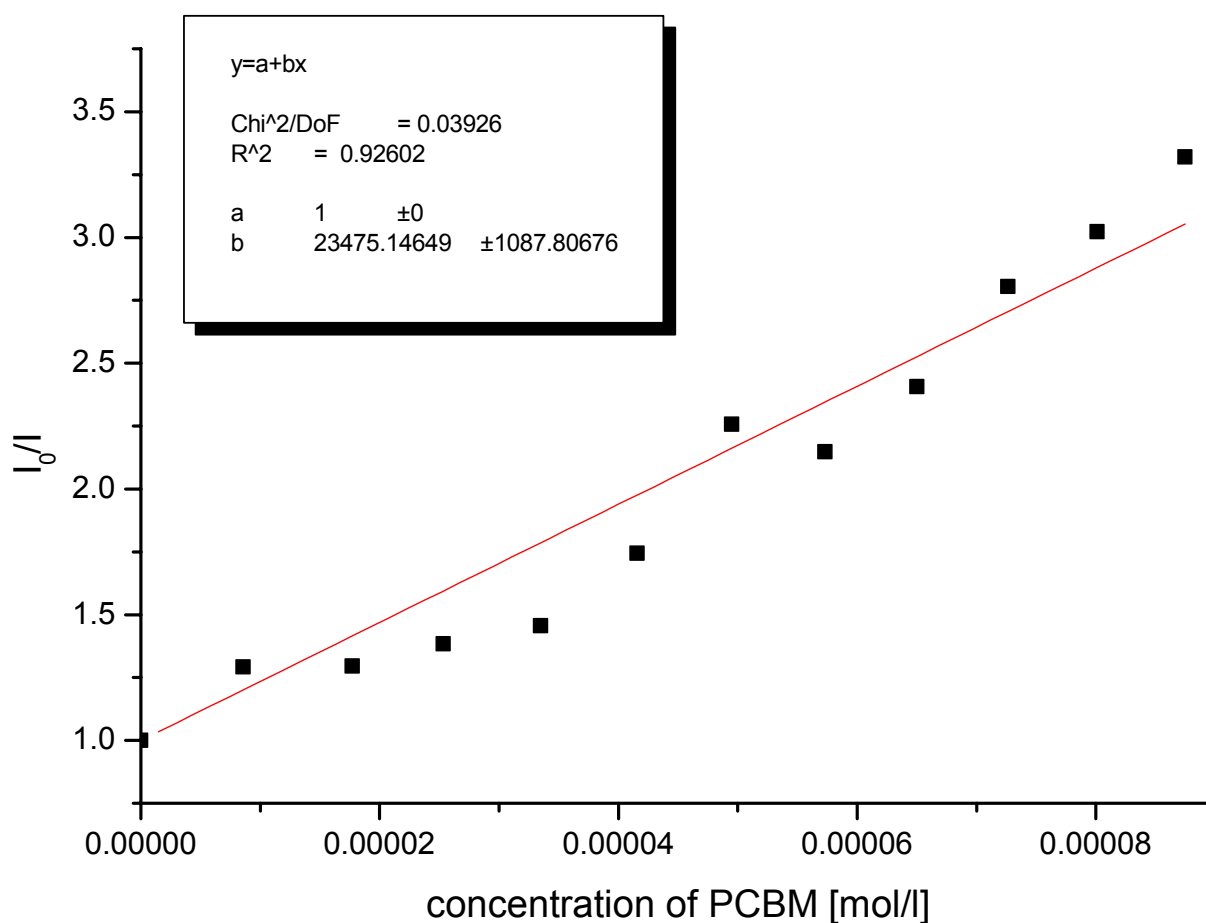
Figure 3. 19 Stern – Volmer plot of P3HT with PCBM

It was proven before that ultra fast electron transfer from this polymer to the fullerene occurs. Therefore the quenching of the photoluminescence can be correlated with this effect. [25,26,31]

It can be derived from Figure 3. 19 that the K_{SV} for P3HT quenched with PCBM is $23x10^3$ l/mol. Together with $\tau_F \approx 500$ ps [25], the P3HT concentration of 0.02 mg/ml and a $M_n \approx 25500$ g/mol [33] this leads to a value of $k_q \approx 4 \times 10^7$ s^{-1}. The given τ_F value is taken from poly(3-octylthiophene) but according to their structural similarity it is assumed that the lifetimes of PL are more or less the same. The M_n value was taken from reference [33] because the company [35] from which the material was purchased uses the synthesis described in this paper and references to it.

3.2.5. ZnPc/TP599 and PCBM

The aim of this experiment was to show that TP 599 forms coordinative bonds over its pyridyl residuals to the zinc in the ZnPc. Therefore TP 599 should be a better quencher for the photoluminescence of ZnPc than PCBM.

3.2.5.1.   ZnPc and PCBM

The ZnPc solution contained 0.1 mg zincphthalocyanine and was diluted 1:4 for the measurement. A pure photoluminescence spectrum was taken and then a 0.1 w% PCBM solution (in toluene) was added stepwise, so that a $4.4 \cdot 10^{-6}$ mol/l, 1.3×10^{-5} mol/l, 2.2×10^{-5} mol/l, 3×10^{-5} mol/l and a 3.8×10^{-5} mol/l PCBM solution was present in the first pure ZnPc solution.

The maps were measured in the wavelength range from 630 to 830 nm. The spectra were taken with 2.5 nm steps, doing 5 shots per step. The bandwidth was set to 1. The voltage range was 1600 mV and the time range 200 ns. The excitation wavelength was 355 nm. To get rid of the second harmonic of the laser at 710 nm both filters were used together. The maximum of the peak is at 677.5 nm. (Figure 3. 20)

Figure 3. 20 Spectra of ZnPc solution with PCBM

For the Stern – Volmer plot the maximum of the peaks at 677.5 nm were take. The x-axis is the molarity of PCBM. (Figure 3. 21)
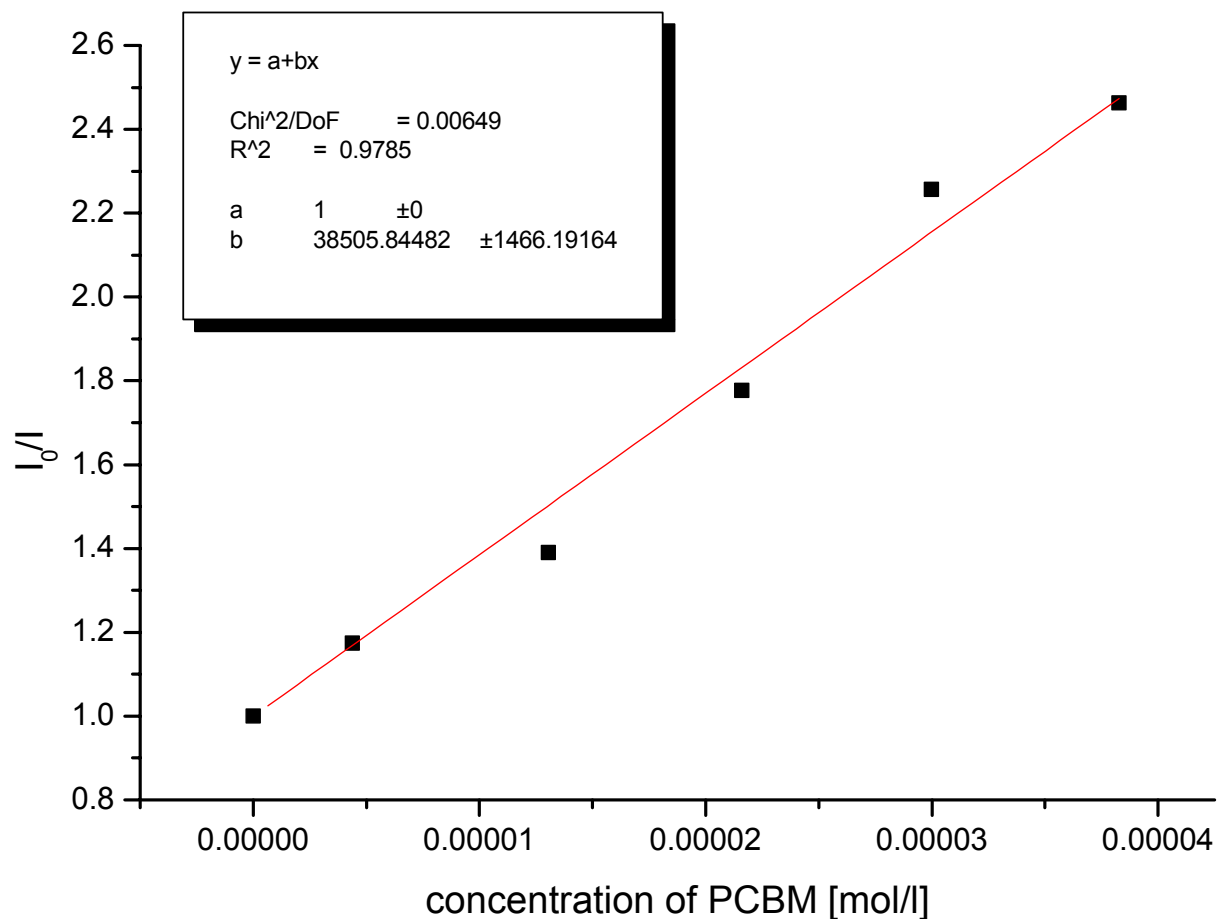
Figure 3. 21 Stern – Volmer plot of ZnPc and PCBM

It can be derived from Figure 3. 21 that the Stern – Volmer constant is $38 \cdot 10^3$ l/mol with PCBM as quencher for the photoluminescence of ZnPc. Together with a $\tau_F \approx 3$ ns [34], a ZnPc concentration of 0.1 mg/ml and M = 577.91 g/mol this leads to a value of $k_q = 2 \times 10^9$ s^{-1}. [24]

3.2.5.2.   ZnPc with TP 599

The ZnPc solution contained 0.1 mg zincphthalocyanine and was diluted 1:4 for the measurement. First of all a pure photoluminescence spectrum was taken and then a 0.1 w% TP599 solution (in toluene) was added so that in the TP599 concentration in the solution was 4×10^{-6} mol/l, 1.1×10^{-5} mol/l ,2×10^{-5} mol/l, 2.7×10^{-5} mol/l, 3.5×10^{-5} mol/l and 5×10^{-5} mol/l.

The maps were measured in the wavelength range from 630 to 830 nm. The spectra were taken with 2.5 nm steps, doing 5 shots per step. The bandwidth was set to 1. The voltage range was 1600 mV and the time range 200 ns. The excitation wavelength was 355 nm. To get rid of the second harmonic of the laser at 710 nm both filters were used together. The maximum of the peak is at 677.5 nm. (Figure 3. 22)
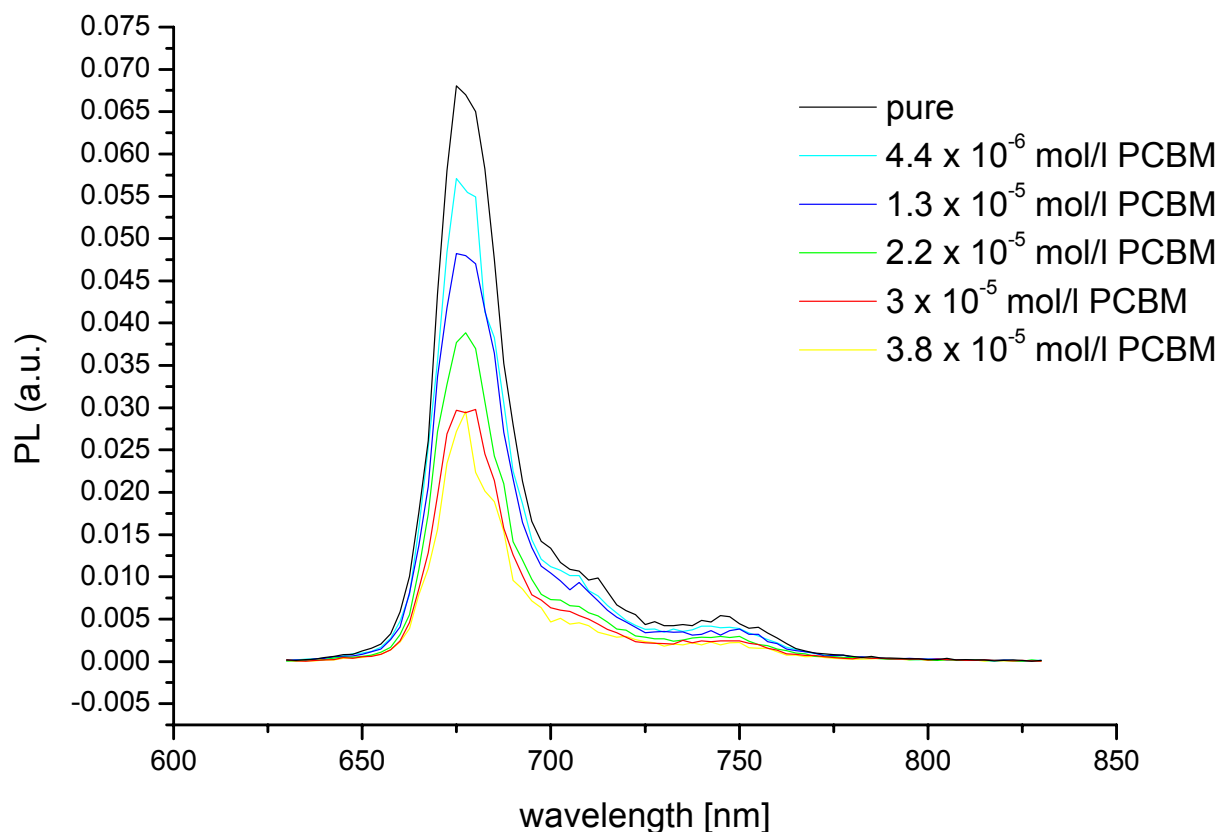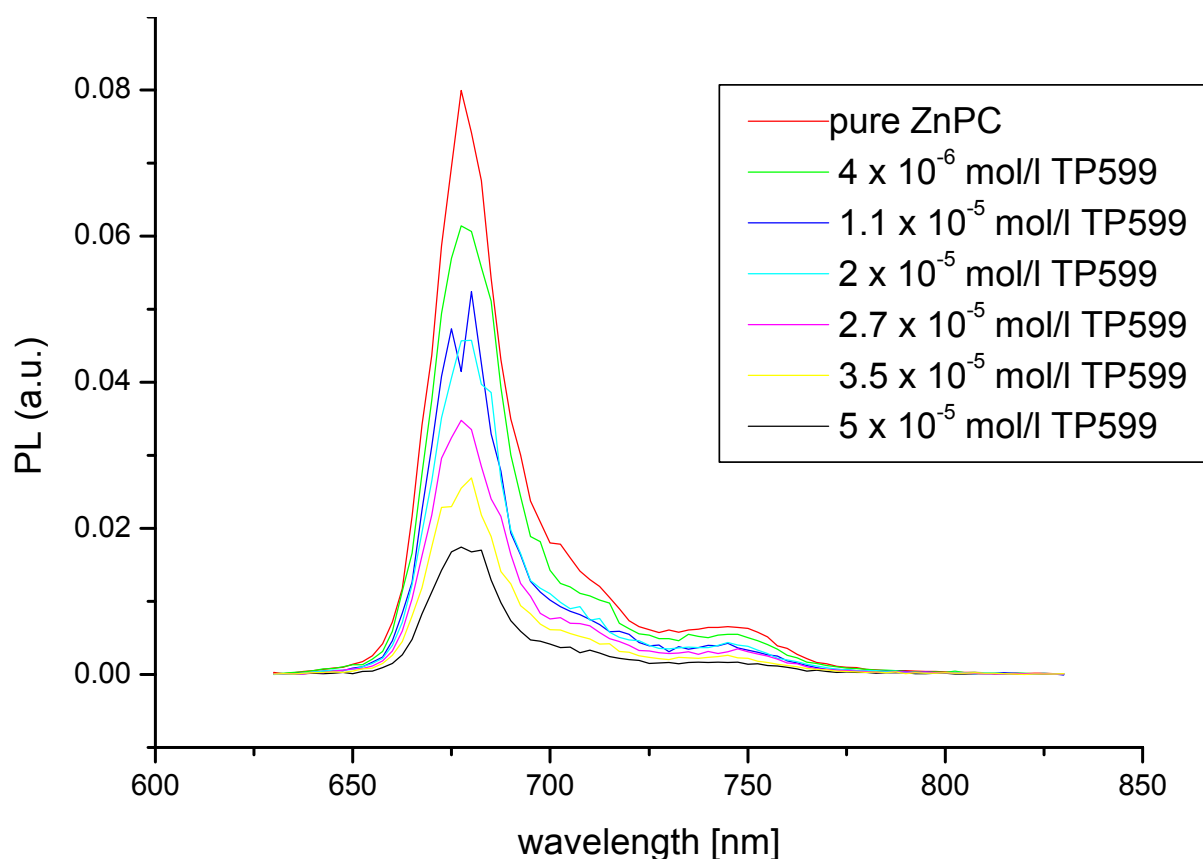

Figure 3. 22 Spectra of ZnPc solution with TP599

Again the value of the peak maximum at 677.5 nm were taken and than plotted in a Stern – Volmer plot where the x – axis is the molarity of TP599.(Figure 3. 23)
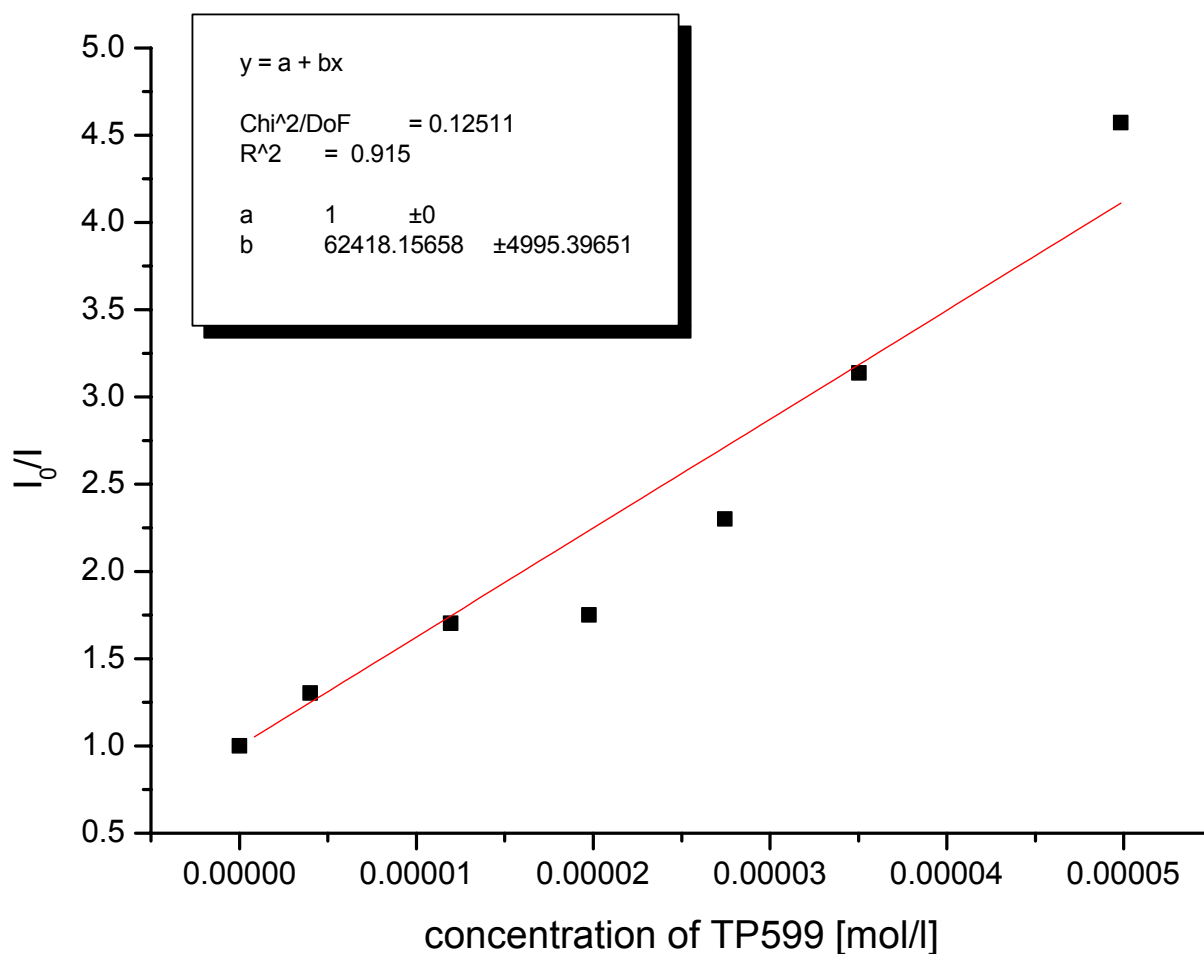
Figure 3. 23 Stern – Volmer plot of ZnPc with TP599

The Stern – Volmer constant for TP 599 as quencher is 62×10^3 l/mol. Together with a $\tau_F \approx 3$ ns [34], a ZnPc concentration of 0.1 mg/ml and M = 577.91 g/mol this leads to a value of $k_q = 4 \times 10^9$ s^{-1}.

3.2.5.3. Comparison of PCBM and TP599

red TP 599 K_{SV} = 62 x 10^3 mol/l k_q = 4 x 10^9 s^{-1}
black PCBM K_{SV} = 38 x 10^3 mol/l k_q = 2 x 10^9 s^{-1}
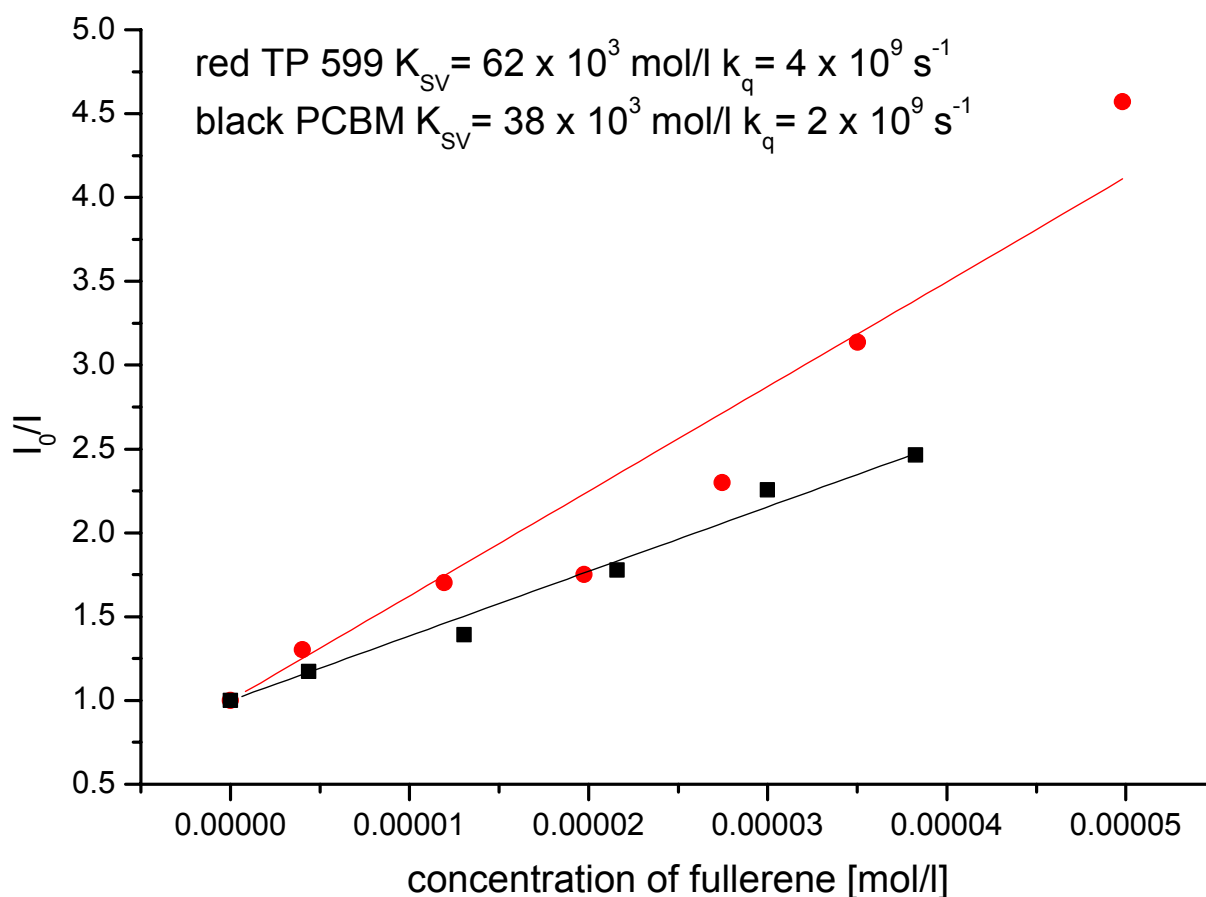
Figure 3. 24 Comparison of PCBM and TP599

If these two fullerenes are compared it appears that TP599 is a better quencher for the ZnPc. There is a hint of a superlinear behaviour of TP 599, whereas PCBM shows a linear behaviour. This superlinear behaviour is a hint that the quenching of the PL is not only diffusion controlled. There might be an additional influence of the coordinative bonds. A proof of this theory could not be given with this experiment because there might be some influence of the solvent on the quenching mechanism (aromatic ring of toluene). Therefore it was decided to look for another solvent for showing that TP 599 quenches the PL better due to coordinative bonds.

3.2.5.4.   Solutions in Dichloromethane

To get rid of the effect of the solvent it was tried to measure the quenching in dichloromethane solution. ZnPc is only soluble in dichloromethane if TP599 is present, this is a hint to the coordinative bond between these two materials. This means that in a solution of ZnPc and TP599 there should be a donor-acceptor complex.

Here it was tried to show the quenching effect the other way round. If TP599 quenches the PL of ZnPc, ZnPc should thus quench the PL of TP 599. Therefore a solution containing 0.1 w% of TP 599 was measured and afterwards a little bit of ZnPc was diluted into this solution and the PL was measured again.

As the signal was rather small the bandwidth was set to 2.5. The map was measured in the wavelength rage from 650 to 820 nm. The voltage range was 16 mV and the time range was 200 ns. The whole map was measured with 2.5 nm steps and each trace was measured 5 times and afterwards averaged.

The spectrum (Figure 3. 25) shows two different peaks one at 677.5 nm (the maximum of the PL of ZnPc) and a second one at 707.5 nm. The second peak at 707.5 nm can be attributed to the maximum of PL peak of TP 599 (Figure 3. 26)
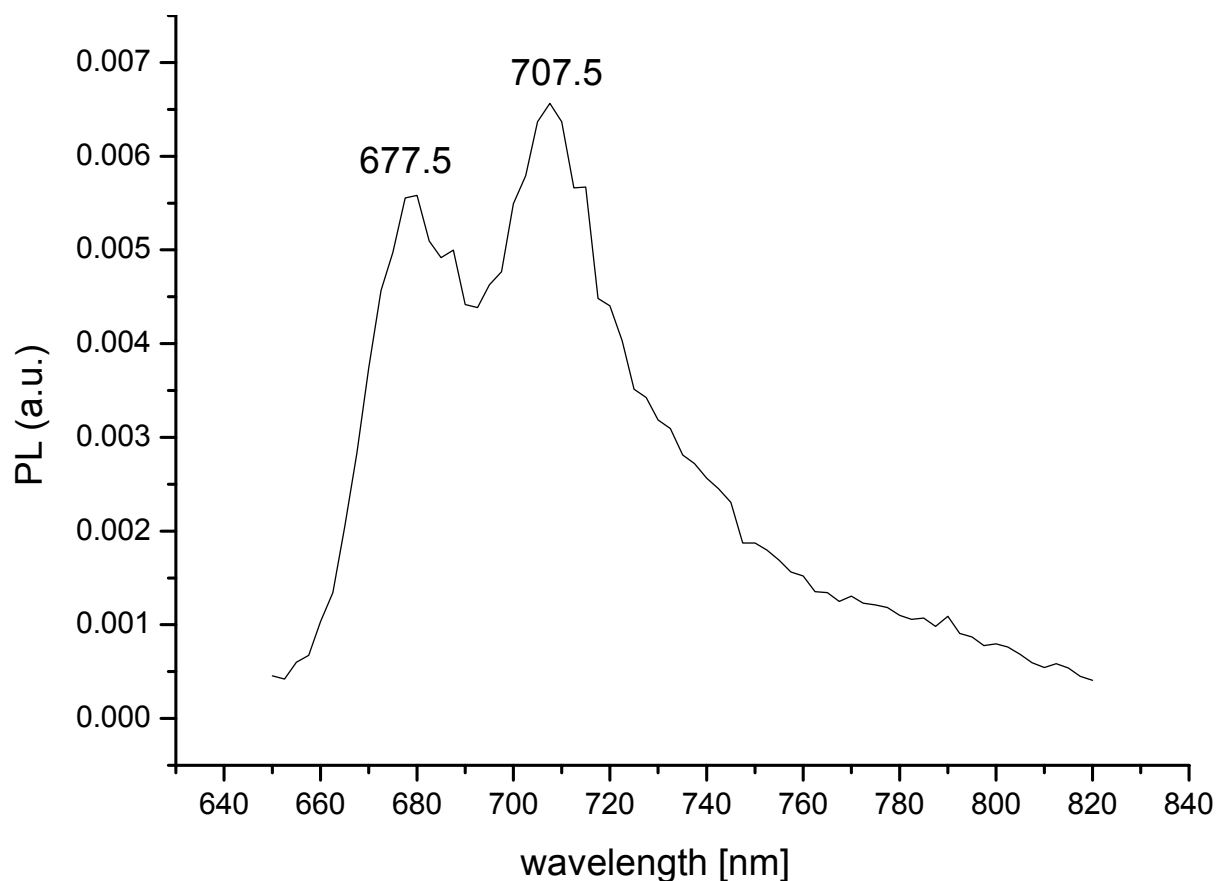

Figure 3. 25 Photoluminescence of TP599 and ZnPc in CH_2Cl_2

60
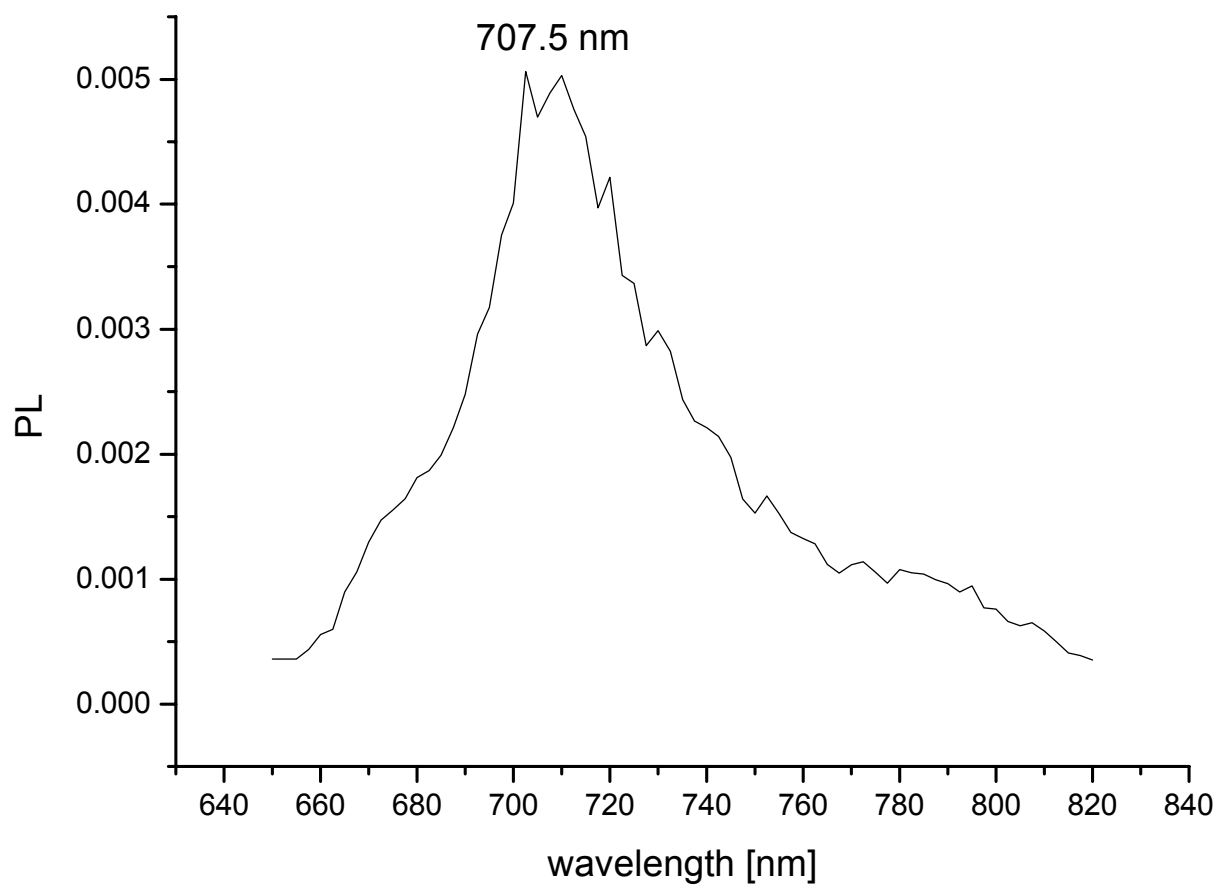
Figure 3. 26 Photoluminescence spectrum of TP599 in dichloromethane solution

The expected strong luminescence quenching of both components could not be observed.

3.2.5.5. ZnPc in chloroform

The third solvent that was tried out was chloroform. First of all it was tried to dissolve ZnPc in chloroform. It showed that some small amount was soluble under the treatment of an ultrasonic bath. After this treatment the solution was filtered. During the filtering process the solution lost a lot from its blue colour, which is an indication that the ZnPc is not fully dissolved.

In the setup measurement to optimize the signal it appeared that the signal decreased over the time. To verify this effect a multiple measurement was carried out. The bandwidth was set to 1 at a wavelength of 677 nm. The time range was 1600 mV and the time range was 200 ns. The measurement was carried out in the 10 Hz mode doing 32 averages. 999 measurements were carried out to follow the decay of the photoluminescence.

The result of this measurement can be seen very clearly in contour plot. (Figure 3. 27) In Figure 3. 28 it can be seen that over the number of scans the signal is decreasing monotonously.

This effect occurs when the solution is exposed to a flash laser light. After leaving the sample in darkness the intensity did not decrease only exposure to laser light led to degradation. Thus it can be assumed that this effect is due to some photochemical process.

$X = 106.00$ (Time / ns)
$Y = 0.00$ (Scans)
$Z = 1.063$ E-2 (Volts)

Figure 3. 27 Contour plot of the multiple measurement of ZnPC in CHCl$_3$

Figure 3. 28 Decay of the photoluminescence of ZnPC over the scans

Chapter 4

4 Conclusion

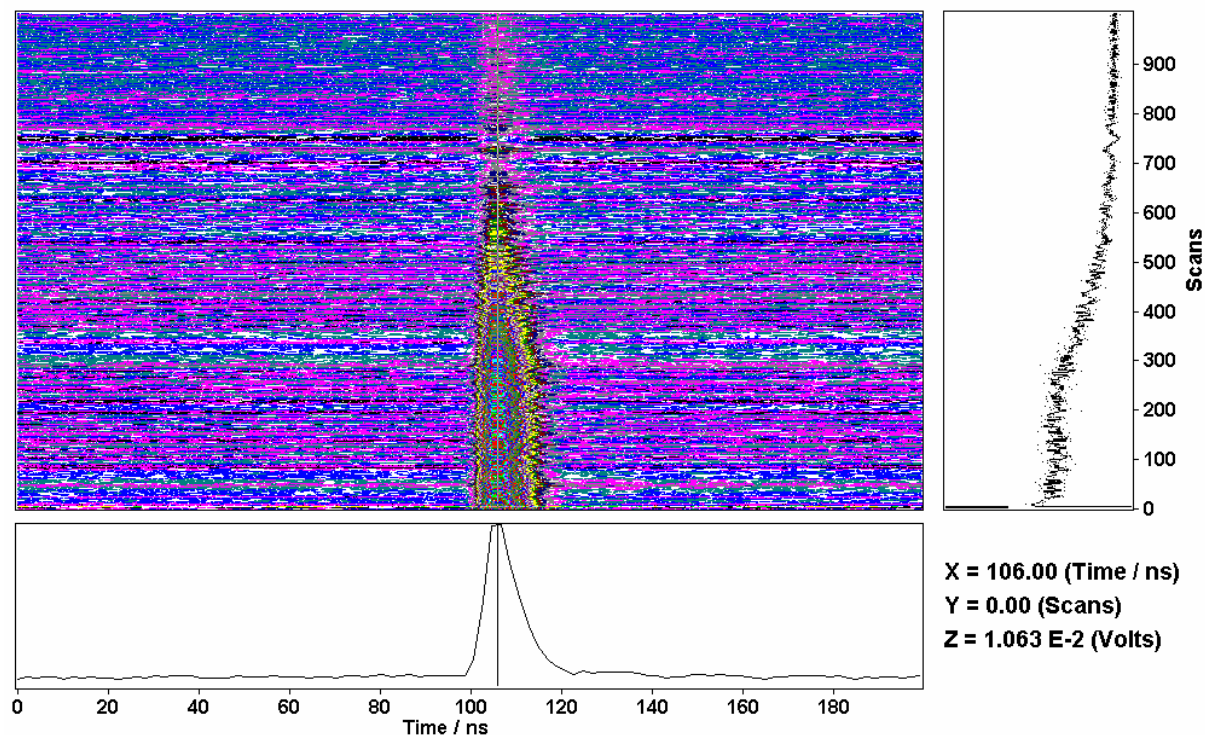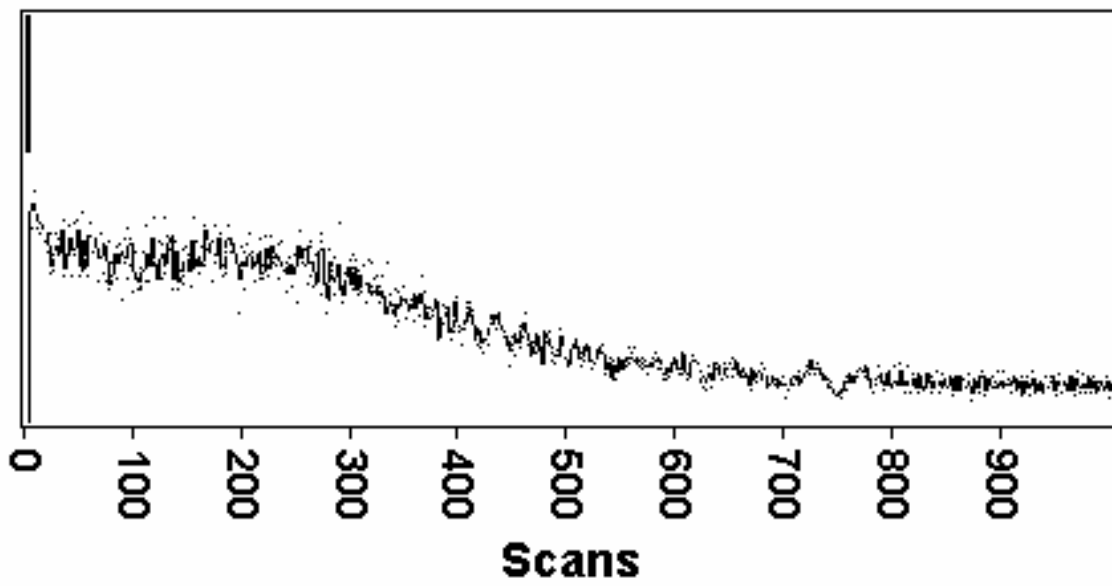The first part of this diploma thesis was the characterization and the optimization of the new LP920 system. The first goal was to understand the complete system and to characterize the different parts of the system.

The first task was the measurement of the wavelength range of the detectors. Therefore the lamp signal was measured with both detectors in the map mode to see until which wavelength the detectors are efficient working. It was found out that the PMT detector covers a wavelength range from 185 to 850 nm and the NIR detector from 850 to 2100 nm. The NIR detector is much less sensitive than the PMT detector. A further important limitation of the system was the saturation limit of the NIR detector. The experiments showed that this is at a signal of 9.6×10^{-2} V.

An important part was the introduction of the ultrafast photodiode to get a reliable trigger signal for the oscilloscope. This improved the 10 Hz measurements with the laser.

To characterize the performance of the irises, an experiment was carried out with opening and closing the different irises. It was found out that in most cases it is the best way to close the iris 1 and 3 to about ¾. This helps avoiding a saturation of the detectors. The iris 2 should be opend fully for the absorption measurements to get a good signal to noise ratio. For photoluminescence measurements one should close this iris to about ¾. This helps getting rid of effects due to scattered laser light especially in the wavelength range of the second harmonic of the excitation.

Introducing the filters to the system reduces the second harmonic scattered laser light significantly.

All the measurements were done on solutions. Film measurements were tried out but no signal could be observed. This results from the design of the sample holder. In the present setup the sample holder is designed in a cross beam geometry, which means that the laser and the probe light intersect in one point. In the case of solutions in a cuvette this is the best design because this point is extended inside the cuvette volume. But for film measurements, the intersecting volume is limited by the film thickness. To get a signal out from this small volume the laser light intensity would have to be increased so far that the films will be damaged or burnt. Therefore a different design of the sample would be more appropriate for film measurements:

the quasi co linear setup. Here the laser light and the probe light intersect in much bigger volume. Therefore it is easier to detect the signal. At the moment this design was not available in combination with a cryostat but will be soon introduced to the LP920 system.

It was found out that the in most cases the best spectra are measured when doing 32 averages in the 10 Hz mode. If the spectra are measured with less than 1 nm steps high noise levels may occur.

The first material measured was a C_{60} solution. Two different kinds of absorption measurements were carried out. The first one in the wavelength range of the T_1 - T_N absorption. The lifetime of the excited state is in the order of the data given in the literature for a solution in which air has diffused in. The second part of the measurement was in the wavelength range for the $T_1 - T_2$ transition. A photoluminescence spectrum of C_{60} could not be observed.

Further investigations were carried out on PCBM solutions. According to the structural similarity of C_{60} and PCBM the absorption spectra are in the same wavelength region. The lifetime of the excited states are much shorter than for the C_{60} sample. This is due to the diffusion of air into the solution because $^3O_2$ is an effective quencher for the triplet state of PCBM.

Two different conjugated polymers were investigated: P3HT and MDMO-PPV. Of both materials the photoluminescence spectra were measured. The lifetimes are in a time range below the time resolution of the LP920 system.

The maximum of the peaks are in the case of P3HT at 579nm and in the case of MDMO – PPV at 620 nm.

The second part of the measurements of the conjugated polymers was to determine the quenching. In both cases the quencher was a PCBM solution which was added stepwise to the solution of the conjugated polymer. After the measurements, the data was plotted as a Stern – Volmer plot. From this plot the K_{SV} and further the k_q values were derived. For the MDMO – PPV K_{SV} is 18×10^3 l/mol and k_q is 4×10^6 s^{-1} and for P3HT it is 23.10^3 l/mol and k_q is 4×10^7 s^{-1}.

A further material combination which was investigated was ZnPc and TP599. It was tried to show that TP599 is a much better quencher for the ZnPc due to coordinative bounds than PCBM. The first try was a solution in toluene. In both cases, for TP599 and PCBM the ZnPc photoluminescence is effectively quenched. The Stern – Volmer constant is higher for the TP599. In addition, a superlinear behaviour of TP 599 was observed which indicates that the

quenching is not only diffusion controlled. This might be due to the complex formation between TP599 and ZnPc.

Therefore a second measurement was carried out with dichloromethane as solvent. The aim of this experiment was to show the effect of ZnPc as a quencher for the TP 599 photoluminescence. But the concentration of ZnPc attainable in the mixed solution was very small, no strong quenching was observable.

The third try was with chloroform. Here the photoluminescence of ZnPc could first be detected but it decreases as an effect of illumination, indicating that there is no stable solution of ZnPc in $ChCl_3$.

References

[1]   P.W. Atkins, *"Molecular Quantum Mechanics 2nd edition"*, Oxford University Press, 1983

[2]   P.W.Atkins, *"Physikalische Chemie"*, VCH, 1988

[3]   G.Porter, *"Flash Photolysis and some of its applications"*, Nobel Lecture, 1967

[4]   P. Suppan, *"Chemistry and Light"*, The Royal Society of Chemistry, 1994

[5]   Operating Instructions LP920 Issue 2, Feburary 2004

[6]   A. Gilbert, J. Baggott *"Essentials of Molecular Photochemistry"*, Blackwell Scientific Publications, 1991

[7]   provided by Dr. Laurance Lutsen, IMEC ,IMOMEC Divison, Belgium

[8]   J.W. Arbogast, A. Darmanyan, C.S. Foote, Y. Rubin, F.N. Diederich, M.M. Alvarez, S. Anz, R.L. Whetten, *J.Phys.Chem,* **95**, 1991, 11-12

[9]   M.S. Dresselhaus, G. Dresselhaus and P.C. Eklund *"Science of Fullerenes and Carbon Nanotubes"*, Academic Press, Inc.,1996

[10]   P.A. Troshin, S.I. Troyanov, G.N. Boiko, R.N. Lyubovskaya, A. Lapshin, N.F. Goldshleger, *Fuller.Nanotub.Car.N.,* **12**, 2004, 413-419

[11]   C. Winder, D. Mühlbachler, H. Neugebauer, N.S. Sariciftci, C. Brabec, R.A.J. Janssen, J. K. Hummelen, *Mol. Cryst. Liq. Cryst.,* **385**, 2002, 93- 100

[12]   L. Smilowitz, A. Hays, A.J. Heeger, J.E. Bowers, *J. Chem. Phys.,* **98**, 1993, 6504-6509

[13] U. Lemmer, R.F. Mahrt, Y. Wada, A. Greiner, H. Bässler, E.O. Göbel, *Appl. Phys. Lett.*, **62**, 1993

[14] V.A. Sautenkov, S.A. van den Berg, G.W. van't Hooft, E.R. Eliel, ???

[15] C.M. Heller, I.H. Campbell, B.K. Laurich, D.L. Smith, D.D.C. Bradley, P.L. Burn, J.P. Ferrairs, K. Müllen, *Phys. Rev. B*, **54**, 1996, 5516-5522

[16] G.R. Hayes, I.D. Samuel, R.T. Phillips, *Phys. Rev. B*, **52**, 1995, 569-572

[17] C.J. Brabec, G. Zerza, G. Cerullo, S. De Silvestri, S. Luzzati, J.C. Hummelen, N.S. Sariciftci, *Chem. Phys. Lett.*, **340**, 2001, 322-326

[18] G. Zerza, C.J. Brabec, G. Cerullo, S. De Silvestri, N.S. Sariciftci, *Chem. Phys. Lett.*, **119**, 2001, 637-638

[19] I. Montanari, A.F. Nogueira, J. Nelson, J.R. Durrant, C. Winder, M.A. Loi, N.S. Sariciftci, C. Brabec, *Appl. Phys. Let.*, **81**, 2002, 3001-3003

[20] A.F. Nogueira, I. Montanari, J. Nelson, C. Winder, N.S. Sariciftci, C. Brabec, J.R. Durrant, *Synthetic Met.*, **137**, 2003, 1505-1506

[21] M. Yan, L.J. Rothberg, F. Papadimitrakopoulos, M.E. Galvin, T.M. Müller, *Phys. Rev. Lett.*, **73**, 1994, 744-747

[22] J.K.J. van Duren, X. Yang, J. Loos, C.W.T. Bulle-Lieuwma, A.B. Sieval, J.C. Hummelen, R.A.J. Janssen, *Adv. Funct. Mater.*, **14**, 2004, 425-434

[23] M.C. Scharber, N.A. Schultz, N.S. Sariciftci, C.J. Brabec, *Phy., Rev. B*, **67**, 2003, 085202-1-085202-7

[24] C. Winder, C. Lungenschmied, G. Matt, N.S. Sariciftci, A.F. Nogueira, I. Montanari, J.R. Durrant, C. Arndt, U. Zhokhavets, G. Gobsch, *Synthetic Met.*, **139**, 2003, 577-580

[25]   N.S. Sariciftci, L. Smilowitz, A.J. Heeger, F. Wudl, *Science*, **258**, 1992, 1474-1476

[26]   C. Winder, N.S. Sariciftci, *J. Mater. Chem.,* **14**, 2004, 1077-1086

[27]   A.F. Nogueria, I. Montanari, J. Nelson, J.R. Durrant, C. Winder, N.S. Sariciftci, C. Barbec, *J. Phys. Chem. B*, **107**, 2003, 1567-1573

[28]   H. Lin, Y. Weng, Q. He, M. Zheng, F. Bai, *Appl. Phys. Let.,* **84**, 2004, 2980 – 2982

[29]   Covion Organic Semiconductors, GmbH

[30]   L. Magnani, R. Rumbles, I.D.W. Samuel, K. Murray, S.C. Morrati, A.B. Holmes, R.H. Friend, *Synthetic Met.,* **84**, 1997, 899-900

[31]   L. Smilowitz, N.S. Sariciftci, R. Wu, C. Gettinger, A.J. Heeger, F. Wudl, *Phys. Rev. B*, **47**, 1993, 13835-13842

[32]   B. Kraabel, D. Moses, A.J. Heeger, *J. Chem. Phys.*, **103**, 1995, 5102-5108

[33]   T.A. Chen, X. Wu, R.D. Rieke, *J. Am. Chem. Soc.,* **117**, 1995, 233-244

[34]   G. Valduga, E. Reddi, G. Jori, R. Cubeddu, P. Taroni, G. Valentini, *J. Photochem. Photobiol. B*, **16**, 1992, 331-340

[35]   Rieke Metals, Inc.

Curriculum Vitae

Name:	Anita Fuchsbauer
Date of birth:	20th March 1980
Birthplace:	Linz
Nationality:	Austrian
Martial Status:	unmarried
Address:	In der Fischerwiesen 5, 4030 Linz
Telephone:	0043-650-8418118
E-mail:	anita.fuchsbauer@jku.at

Education

04/2004 – 06/2005	Diploma Thesis at the institute of physical chemistry
10/1998 – 07/2005	Studies at the University of Linz: technical chemistry
06/1998	School leaving exam passed with distinction
	Scholary paper in biology
	Mag. Windischofer
	"Die Muskulatur des Menschen und ihre Bedeutung für die Körperhaltung"
1995-1998:	Grammar school : Adalbert Stiftergymnasium ORG der Diözese Linz
1990-1995:	Secondary School: PMHS der Brucknerschwestern in Linz
1985-1990:	Primary School in Linz Kleinmünchen

Related Experience

10/2004-06/2005	tutor for "Übung aus Physikalischer Chemie I und II" at the Institute of Physical Chemistry at the University of Linz
03/2005	Nanochannel spring school in Brigels, Switzerland
07/2004	Schooling of the LP920 system at the TU Eindhoven, Netherlands
08/2003-09/2003	project collaborator at the institute of physical chemistry

Further Employers

11/2001-09/2002	FIT (Frauen in die Technik) project at the University of Linz
09/2000-09/2001	Borealis

Additional Experience

07/2003	Spanish course in Barcelona, Spain
07/2002	Spanish course in Canet, Spain
09/2001	Spanish course in Denia, Spain

Additional Qualification

Language:	English (fluent), German (mother tongue). Spanish (beginner)
Computer:	MS Word, MS Excel, Origin
Drivers licence:	since 1998 (A and B)

Hobbies

Ice hockey, inline hockey, skiing, travelling

EIDESSTATTLICHE ERKLÄRUNG

Ich erkläre an Eides statt, dass ich die vorliegende Diplomarbeit selbständig und ohne fremde Hilfe verfasst, andere als die angegebenen Quellen und Hilfsmittel nicht benutzt bzw. wörtlich oder sinngemäß entnommene Stellen als solche kenntlich gemacht habe.

Linz, den ……………..   ………………………………………...

                                                    (Unterschrift)